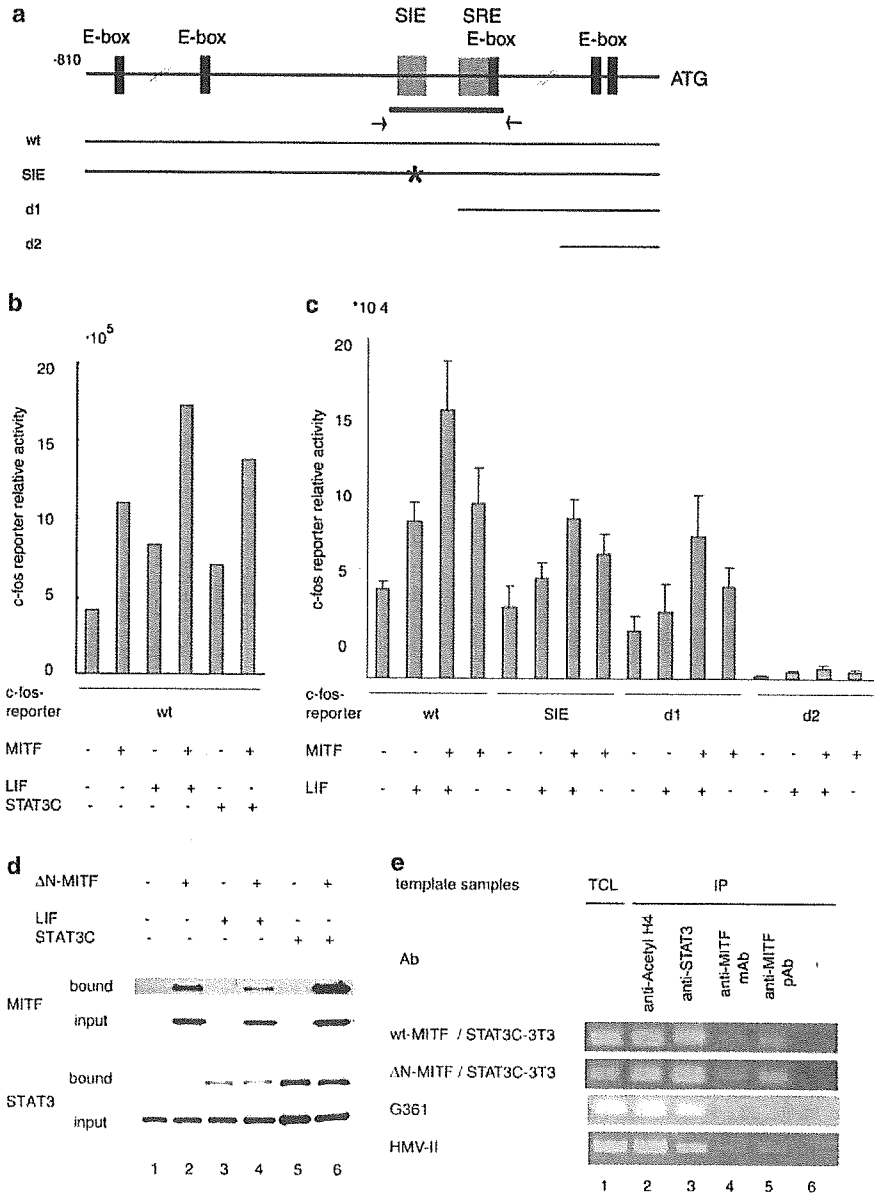

Figure 5 MITF and STAT3C directly binds to the promoter region of c-fos. (**a**) A diagram of the c-*fos*-luciferase reporter gene containing five E-boxes, potential MITF-binding motifs, and the SIE region known as a binding site of STAT3. Asterisks indicate mutations in SIE, and two deletion mutants (d1 and d2) are shown. The bold bar shows the region used for the DNA-binding assay and arrows show the PCR primers for ChIP assay. (**b** and **c**) *Reporter assay*. HEK293 cells were transfected with a plasmid mixture containing the c-*fos*-luciferase reporter gene (2 ng), the *β*-galactosidase gene (0.1 *μ*g), STAT3C (0.2 *μ*g), and the wt-MITF plasmid (**b**, 200 ng, and **c**, 10 ng). After transfection, cells were incubated in the presence or absence of 10 ng/ml LIF for 8 h, and cell extracts were prepared. Data normalized with the *β*-galactosidase activity from triplicate experiments are shown. (**d**) *DNA-binding assay*. 293T cells were transfected with the pcDNA3-Myc-ΔN-MITF and pRcCMV-STAT3C and stimulated with 10 ng/ml LIF for 6 h, and the nuclear extracts were prepared. The DNA-binding proteins bound to the oligonucleotide-conjugated beads were analysed by immunoblotting with anti-STAT3 and anti-Myc antibodies. (**e**) ChIP assay was performed to determine the binding of MITF and STAT3 to the promoter region of c-*fos*. wt- or ΔN-MITF-infected STAT3C-3T3 was determined *in vitro*, and the melanoma cells G361 and HMV-II were examined *in vivo*. Chromatin complexes were immunoprecipitated with anti-acetylated histone H4, anti-STAT3, and monoclonal or polyclonal anti-MITF antibodies

significantly suppressed the anchorage-independent growth of wt- or ΔN-MITF-infected STAT3C-3T3 cells. These data support our notion that c-*fos* induction is one of the mechanisms of increased anchorage-independent growth of MITF/STAT3C-expressing cells.

colony formation efficiency (%)

	retrovirus infection	wt-MITF	ΔN-MITF
colonies (size)			
> 0.3 mm	-	1.30 ± 0.28	10.85 ± 1.55
	cont.	1.11 ± 0.41	6.83 ± 3.31
	dnAP-1	0.03 ± 0.05	1.33 ± 0.90
0.1 mm - 0.3 mm	-	6.40 ± 1.26	-
	cont.	4.98 ± 1.88	-
	dnAP-1	0.84 ± 0.88	-

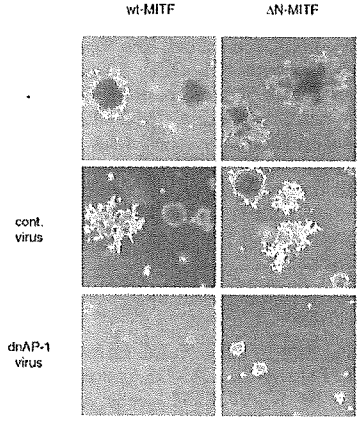

Figure 6 Expression of dominant-negative AP-1 inhibits anchorage-independent growth of MITF/STAT3C-expressing cells. wt- or ΔN-MITF-infected STAT3C-3T3 cells were infected with retrovirus carrying dominant-negative AP-1 (dnAP-1) or an empty vector by the retrovirus at moi = 10. Cells were selected with puromycin and then plated into soft-agar medium. On day 21, colonies were counted and photographed. Data from triplicate experiments are shown

Discussion

In this study, we identified MITF as a collaborative factor of STAT3 for cellular transformation. Many factors have been shown to interact with and activate (or in some cases inactivate) STAT3. For example, we have shown that the HCV core protein directly interacts with STAT3 and induces phosphorylation and activation (Yoshida *et al.*, 2002). Nakayama *et al.* (2002) reported that a nuclear zinc-finger protein EZI enhances the nuclear retention and transactivation of STAT3. PIAS3 (Levy *et al.*, 2002), cyclinD (Matsui *et al.*, 2002), and GRIM-19 (Lufei *et al.*, 2003) also interact directly with STAT3, but inhibit transcriptional activity. Most of these factors are isolated as a physical binding protein with STAT3. In this study, by using functional expression screening, we showed that STAT3 and MITF interact functionally, but not physically. A common target of STAT3 and MITF is found to be c-*fos*, which may participate in transformation by constitutively active STAT3 and MITF. Our functional cloning strategy using retroviral cDNA transfer will provide an additional candidate for the cofactor that modulates the function of STAT3. Furthermore, in this study we demonstrated that the microarray technique is a powerful tool to identify a target gene that is cooperatively induced by two distinct classes of transcription factors.

MITF consists of at least five isoforms, MITF-A, MITF-B, MITF-C, MITF-H, and MITF-M, differing at their N-termini and expression patterns (Tachibana, 1997; Udono *et al.*, 2000; Shibahara *et al.*, 2001). However, the clone (ΔN-MITF) we obtained from the HeLa cell library has an N-terminal deletion, which is shorter than other reported forms. Since mRNA corresponding to ΔN-MITF has not been reported, we speculate that ΔN-MITF is a product of the incomplete elongation of cDNA by reverse transcriptase. Nevertheless, ΔN-MITF seems to be a more potent inducer for a transformed phenotype of NIH-3T3 cells (Figure 1) and c-*fos* induction (Figure 4). In addition to the previously characterized acidic activation domain necessary for melanocyte differentiation, a second potential activation domain is shown to be located between amino acids 140 and 185 (Mansky *et al.*, 2002), and ΔN-MITF contains these regions. Therefore, the N-terminal, with about 100 amino acids of MITF-M, may be a negative regulatory domain. This region contains a glutamine-rich basic region (QB), but the function of this region has not been elucidated. Most notably, Ser 73 of MITF-M is a predicted MAP kinase-phosphorylation site and is implicated in p300/CBP recruitment (Hemesath *et al.*, 1998) and reduced MITF protein stability (Kim *et al.*, 2003). Since ΔN-MITF lacks this Ser 73, dN-MITF may be more stable than wt-MITF.

Several types of functional interactions between STAT3 and MITF have been proposed. The protein inhibitor of activated STAT3 (PIAS3) has been shown to bind to a b-HLH-Zip domain of MITF, resulting in the suppression of MITF-induced transcriptional activity (Levy *et al.*, 2002). However, it has been reported that STAT3 does not interfere, either *in vitro* or *in vivo*, with the interaction between PIAS3 and MITF. This finding is consistent with our data showing that STAT3 does not affect MITF transcriptional activity (data not shown) and MITF does not interfere with STAT3 transcriptional activity (Figure 3c). Recently, Kamaraju *et al.* (2002) reported that IL-6 receptor/IL-6 chimera induces a loss of melanogenesis preceded by a sharp decrease in MITF mRNA and gene promoter activity in B16/F10.9 melanoma cells. IL6RIL6 stimulates gp130, leading to the rapid activation of STAT3, which downregulates Pax3, a paired homeodomain factor regulating MITF mRNA levels and the development of melanocytes. Therefore, in this case, MITF downregulation by STAT3 is indirect, and the mechanism of Pax3 downregulation by STAT3 is not clear. The Pax3 downregulation in IL6RIL6-induced F10.9 cells leads to growth arrest and transdifferentiation to a glial cell phenotype. Therefore, the genetic interaction between MITF and STAT3 seems to be complicated and probably different among cell types.

We found that the c-*fos* gene is a common target of STAT3 and MITF, which probably contributes to transformation. Microarray analysis also revealed that

the c-*fos* gene is strongly upregulated by MITF in primary melanocytes (McGill *et al.*, 2002). In agreement with this notion, STAT3 was frequently phosphorylated in several human melanoma cell lines (Figure 3a). However, while B16 and SKMel cells are negative for STAT3 phosphorylation, the same cells do express c-*fos*. Apparently, STAT3-independent mechanism of c-*fos* induction is present in these melanoma cells. Finding such mechanisms of c-*fos* expression in these cells may provide a new clue for understanding the role of c-*fos* for the generation of melanomas.

Promoter analysis and ChIP assay indicated that STAT3 and MITF can bind to the c-*fos* promoter and activate this promoter independently. Reporter gene analysis suggested that the effect of MITF and STAT3 on the c-*fos* promoter are additive rather than cooperative (Figure 5b). This is consistent with our observation that there is no direct physical interaction between MITF and STAT3. Nevertheless, high levels of c-*fos* expression and transformation of NIH-3T3 cells are dependent on both STAT3 and MITF. In addition to promoter activation, another mechanism of c-*fos* expression, such as stabilization of c-*fos* mRNA, may present in the cooperative effect of STAT3 and MITF. Furthermore, a previous report demonstrated that wt- and mi-MITF bind to the c-Fos protein. In particular, mi-MITF prevents c-Fos from being transported to the nucleus, and this may be a reason for the osteopetrosis of mi/mi mutant mice (Sato *et al.*, 1999). wt-MITF was also shown to bind to c-Jun and enhance the transactivation of the MMCP-7 gene, while complexes of mi-MITF and c-Jun were predominantly found in the cytoplasm and suppressed transactivation (Ogihara *et al.*, 2001). Thus, MITF could be involved in AP-1 activation not only by inducing c-*fos* but also by interacting with AP-1 itself. The fact that a dominant-negative AP-1 (SupJunD) suppressed colony formation of transformants expressing both MITF and STAT3C suggests that AP-1 can be a therapeutic target of melanoma.

In addition to c-*fos*, we found several interesting genes that are cooperatively induced by STAT3 and MITF (Figure 4a). GTP cyclohydrase-1 and mast cell proteases are probably involved in melanocyte and mast cell functions. PMEL17 is also known as an MITF-inducible pigment cell-specific gene and a melanosomal matrix protein, which may function as a structural protein in melanogenesis (Kobayashi *et al.*, 1994). JE and A7 are chemokines that are induced by immunoglobulin (Ig) E plus antigen stimulation in mast cells. (Burd *et al.*, 1989; Kulmburg *et al.*, 1992; Ong *et al.*, 1993). Therefore, STAT3/MITF target genes are strongly linked to the function of mast cells and melanocytes, which constitutively express MITF. This finding implies that STAT3 (or other STATs) may be involved in mast cell and melanocyte functions by inducing genes in cooperation with MITF. It is interesting that IL3, which activates STAT5, is a mast cell growth factor *in vitro*. The functions of STATs in mast cells and melanocytes are under investigation.

Materials and methods

Cell culture and transfection

NIH3T3 and HEK293 cells were cultured in Dulbecco's modified Eagle's medium supplemented with 10% CS. STAT3C-transformed 3T3 (STAT3C-3T3) cells (Yoshida *et al.*, 2002) were cultured in DMEM supplemented with 10% CS containing 0.8 mg/ml G418. PLAT-E, a packaging cell line (Morita *et al.*, 2000) was maintained in DMEM with 10% FCS containing blasticidin S (10 mg/ml) and puromycin (1 mg/ml). Melanoma cell lines were cultured in the following medium containing 10% FCS, B16 and B16F10 in RPMI 1640, G361 and SKMel28 in MEM, HMV-II in Ham's F12, and MMAc in DMEM. MC9, a mast cell line, was cultured in RPMI 1640 supplemented with 5% FCS, 50 μM 2-mercaptoethanol, and 6 ng/ml mouse recombinant IL-3. Cells were transfected by the calcium phosphate method with Cell Phect (Amersham) or by the lipofection method with FuGENE 6 (Roche). For retrovirus-mediated gene expression, NIH3T3 cells were infected with the retroviruses produced by PLAT-E as reported (Sasaki *et al.*, 2003). B16, B16F10, G361, and SKMel 28 cell lines were kindly provided by Dr Yonemitsu (Kyushu University, Japan).

Library screening

Retroviruses containing the human HeLa retroviral cDNA library (CLONTECH, Palo Alto, CA, USA) were produced from PLAT-E and 1×10^6 STAT3C-3T3 cells were infected with 10 ml of the retroviral supernatant containing 10 mg/ml polybrene. After 48 h of virus transduction, STAT3C-3T3 cells were seeded in soft-agar medium. Within 3 weeks, two colonies were picked up and expanded, and genomic DNA was isolated. Integrated cDNAs were recovered by PCR using a pair of primers (FWD, 5′-AGCCCTCACTCCTTCTCTAG, and REV, 5′-ATGGCGTTACTTAAGCTAGCTTGC-CAAACCTAC) and sequenced.

Colony formation in soft-agar

The MITF-infected 3T3 and STAT3C-3T3 cells were seeded into 35-mm dishes in suspensions of 0.36% Agar noble (Difco) in DMEM supplemented with 10% CS on top of a bed of 0.72% Agar noble in the same complete medium. The MITF-infected STAT3C-3T3 cells were inoculated with a retrovirus of dominant-negative AP-1 or an empty vector (Ui *et al.*, 2000), selected with puromycin, and plated into soft-agar medium. The cultures were incubated for 21 days and then the colonies were counted and photographed.

Construction of MITF

The cDNAs of wt-, ΔN-, and mi-MITF were subcloned into a bicistronic retrovirus vector pMX-IRES-EGFP (Nosaka *et al.*, 1999) or a pcDNA3 expression vector.

Retrovirus of dominant-negative AP-1

The control virus (pBabe-IRESpuro) and the SupJunD-1 virus (pBabe-SupJunD-1-IRESpuro) as a dominant-negative AP-1 were generated as described (Ui *et al.*, 2000). After infection, STAT3C-3T3 cells were cultured with 2 mg/ml puromycin.

High-density oligonucleotide microarray analysis

RNA was extracted by standard methods. Cells were lysed directly in their Petri dishes in TRIzol reagent (Invitrogen, Carlsbad, CA, USA) and total RNA was isolated according to

the manufacturer's instructions. cRNA preparation and microarray hybridization were carried out according to the supplier's instructions (Affymetrix, Santa Clara, CA, USA), using Genechip HG-U95Av2. Scanned output files were analysed by the probe level analysis package, Microarray Suite MAS 5.0 (Affymetrix, Santa Clara, CA, USA). The signal for each of these genes was determined from the 'probe set' in use for this gene and by the probe level analysis method provided by Affymetrix software.

Northern Blotting analysis and RT–PCR

Total RNA (10 μg) extracted from cells using TRIzol was evaluated by Northern blotting analysis with digoxigenin-labeled antisense RNA of c-*fos* and G3PDH labeled with the DIG RNA Labeling Kit (Roche). To determine the microarray data, 1 μg of total RNA was reverse-transcribed with the Reverse Transcribed Kit (Roche) and RT–PCR was performed with primers as follows: mouse MITF, 5′-GGAACAGCAAC-GAGCTAAGG and 5′-TGATGATCCGATTCACCAGA; human MITF, 5′-AGAACAGCAACGCGCAAAAGAAC and TGATGATCCGATTCACCAAATCTG; mouse GTP cyclohydrorase, 5′-GGCTGCTTACTCGTCCATTC and AG GTGATGCTCACACATGGA; mouse JE, AGGTCCCTGT CATGCTTCTG and TCTGGACCCATTCCTTCTTG; mouse PMEL17 CAGGGGTCTAACTGCTGGAG and TT CGGAGGTTTAGGACCAGA; mouse MRP8, GGAAAT CACCATGCCCTCTA and TGGCTGTCTTTGTGAGAT GC; mouse MARC, TCTGTGCCTGCTGCTCATAG and CTTTGGAGTTGGGGTTTTCA; and mouse MCPL, GCA CTTCTCTTGCCTTCTGG and TGTGCAGCAGTCATCA CAAA.

Western blotting analysis

Cells were lysed in a lysis buffer (50 mM Tris-HCl pH 7.4, 150 mM NaCl, 0.5% or 1% NP-40, 1 mM EDTA, 1 mM vanadate, 50 mM NaF, 1 mM DTT, 0.01 mM APMSF) and centrifuged at 12 000 *g* for 10 min. The supernatants were resolved on SDS–PAGE of 10% gels, blotted, and immunostained with an anti-phospho STAT3 (Tyr705) polyclonal antibody (Cell Signaling Technology) and an anti-STAT3 polyclonal antibody (Santa Cruz Biotechnology).

Luciferase assay

An APRE-luciferase reporter gene for STAT3 activity and a reporter gene construct containing MITF-responsive mMCP-6 (mouse mast cell protease) luciferase have been described previously (Morii *et al*., 1996; Yasukawa *et al*., 1999). A c-*fos* promoter–reporter gene consisting of the c-*fos* promoter region containing SIE, SRE, and several potential MITF-binding motifs (Tsujimura *et al*., 1996) is also described (Shibuya *et al*., 1994; Kawahara *et al*., 1995; Kim *et al*., 1998). Luciferase assays were carried out using the dual-luciferase reporter system (Promega). The expression plasmid of STAT3-C in pRcCMV was kindly provided by Dr JE Darnell Jr (Bromberg *et al*., 1999).

Nuclear extract preparation and oligonucleotide-binding assay

293T cells (1.5×10^7) were transfected with Myc-ΔN-MITF and STAT3C were stimulate with LIF for 6 h. Cells were collected and resuspended in 0.4 ml of buffer A (10 mM HEPES-KOH (pH 7.8), 10 mM KCl, 0.1 mM EDTA, 0.4% NP-40, 1 mM DTT, 0.5 mM APMSF, 2 μg/ml leupeptin, and 1 mM Na_3VO_4). After a brief vortexing and centrifugation, the supernatant was discarded and the nuclei-containing pellet was resuspended in 0.05 ml of buffer C (50 mM HEPES-KOH (pH 7.8), 420 mM NaCl, 5 mM $MgCl_2$, 0.1 mM EDTA, 2% glycerol, 1 mM DTT, 0.5 mM APMSF, 2 μg/ml leupeptin, and 1 mM Na_3VO_4) at 4°C for 30 min. The suspension was pelleted by centrifugation and the supernatants were collected and stored at −80°C until use. Oligonucleotide-conjugated beads were prepared using the DNA-binding protein purification kit (Roche) according to the manufacturer's protocol. In brief, the sense and antisense oligonucleotide of the human c-*fos* promoter sequence, including the SIE and SRE regions (5′-C AGTTCCCGTCAATCCCTCCCCCCTTACACAGGATGTC CATATTAGGACATCTGC-3′) were annealed, and they were ligated with the washed streptavidin magnetic particles for 30 min at 25°C. After ligation was carried out, the particles were washed using a magnetic separator and mixed with 100 μg of the nuclear extract for 30 min at 25°C. Then, the particles were washed and the DNA-binding proteins were eluted. The elutates were pelleted with trichloroacetic acid solution, and analysed by immunoblotting with anti-STAT3 and anti-Myc antibodies.

ChIP assay

For ChIP assay, 243T cells (5×10^6) were fixed with 1% formaldehyde for 10 min at 37°C, washed with PBS, and lysed in ChIP lysis buffer (Upstate Biotechnology, Lake Placid, NY, USA). DNA was sonicated by pulsing five times. Anti-acetylated histone H4 (Upstate), anti-STAT3 (Sigma), or anti-MITF monoclonal antibody (Oncogene), and anti-MITF polyclonal antibody (Santa Cruz Biotechnology) was added (5 μg–20 μg per immunoprecipitation) and incubated overnight. Protein A–agarose beads (Upstate Biotechnology) were added for 1 h and then washed once each with a low-salt buffer, high-salt buffer, and LiCl buffer. They were then washed twice with a TE buffer. The beads were eluted with 0.1 M NaHCO3 and 1% SDS, and crosslinks were reversed at 65°C. DNA was ethanol precipitated in the presence of 20 μg glycogen. PCR was carried out using primers specific to the promoter region of mouse c-*fos* (FWD, 5′-TCTGCCTTTCCCGCCTCCCC, and REV, 5′-GGCCGTGGAAACCTGCTGAC) for NIH3T3, and human c-fos (FWD, 5′-CCCGACCTCGGGAACAAGGG, and REV, 5′-ATGAGGGGTTTCGGGGATGG) for HMV-II, or (FWD, 5′-TCTCATTCTGCGCCGTTCCC, and REV, 5′-GGCCGTGGAAACCTGCTGAC) for G361.

Acknowledgements
We thank Dr T Yoshida (Kurume University) for STAT3C-3T3, Dr Yonemitsu (Kyushu University) for melanoma cell lines, H Meguro for oligonucleotide microarray analysis, Y Kawabata for technical assistance, and N Arifuku for manuscript preparation. This work was supported by special grants-in-aid from the Ministry of Education, Science, Technology, Sports, and Culture of Japan, the Japan Health Science Foundation, the Human Frontier Science Program, the Japan Research Foundation for Clinical Pharmacology, Haraguchi Memorial foundation, and the Uehara Memorial Foundation. AJ is supported by the fellowship from Japan Society for Promotion of Science.

References

Bowman T, Garcia R, Turkson J and Jove R. (2000). *Oncogene*, **19**, 2474–2488.

Bromberg J and Darnell Jr JE. (2000). *Oncogene*, **19**, 2468–2473.

Bromberg JF, Wrzeszczynska MH, Devgan G, Zhao Y, Pestell RG, Albanese C and Darnell Jr JE. (1999). *Cell*, **98**, 295–303.

Burd PR, Rogers HW, Gordon JR, Martin CA, Jayaraman S, Wilson SD, Dvorak AM, Galli SJ and Dorf ME. (1989). *J. Exp. Med.*, **170**, 245–257.

Carreira S, Liu B and Goding CR. (2000). *J. Biol. Chem.*, **275**, 21920–21927.

Darnell Jr JE. (1997). *Science*, **277**, 1630–1635.

Hatakeyama M, Kawahara A, Mori H, Shibuya H and Taniguchi T. (1992). *Proc. Natl. Acad. Sci. USA*, **89**, 2022–2026.

Hemesath TJ, Price ER, Takemoto C, Badalian T and Fisher DE. (1998). *Nature*, **391**, 298–301.

Kamaraju AK, Bertolotto C, Chebath J and Revel M. (2002). *J. Biol. Chem.*, **277**, 15132–15141.

Kawahara A, Minami Y, Miyazaki T, Ihle JN and Taniguchi T. (1995). *Proc. Natl. Acad. Sci. USA*, **92**, 8724–8728.

Kim DW, Cheriyath V, Roy AL and Cochran BH. (1998). *Mol. Cell. Biol.*, **18**, 3310–3320.

Kim DS, Hwang ES, Lee JE, Kim SY, Kwon SB and Park KC. (2003). *J. Cell Sci.*, **116**, 1699–1706.

Kitamura Y, Morii E, Jippo T and Ito A. (2002). *Mol. Immunol.*, **38**, 1173.

Kitamura T, Onishi M, Kinoshita S, Shibuya A, Miyajima A and Nolan GP. (1995). *Proc. Natl. Acad. Sci. USA*, **92**, 9146–9150.

Kobayashi T, Urabe K, Orlow SJ, Higashi K, Imokawa G, Kwon BS, Potterf B and Hearing VJ. (1994). *J. Biol. Chem.*, **269**, 29198–29205.

Kulmburg PA, Huber NE, Scheer BJ, Wrann M and Baumruker T. (1992). *J. Exp. Med.*, **176**, 1773–1778.

Levy C, Nechushtan H and Razin E. (2002). *J. Biol. Chem.*, **277**, 1962–1966.

Lufei C, Ma J, Huang G, Zhang T, Novotny-Diermayr V, Ong CT and Cao X. (2003). *EMBO J.*, **22**, 1325–1335.

Mansky KC, Marfatia K, Purdom GH, Luchin A, Hume DA and Ostrowski MC. (2002). *J. Leukocyte Biol.*, **71**, 295–303.

Matsui T, Kinoshita T, Hirano T, Yokota T and Miyajima A. (2002). *J. Biol. Chem.*, **277**, 36167–36173.

McGill GG, Horstmann M, Widlund HR, Du J, Motyckova G, Nishimura EK, Lin YL, Ramaswamy S, Avery W, Ding HF, Jordan SA, Jackson IJ, Korsmeyer SJ, Golub TR and Fisher DE. (2002). *Cell*, **109**, 707–718.

Morii E, Tsujimura T, Jippo T, Hashimoto K, Takebayashi K, Tsujino K, Nomura S, Yamamoto M and Kitamura Y. (1996). *Blood*, **88**, 2488–2494.

Morita S, Kojima T and Kitamura T. (2000). *Gene Therapy*, **7**, 1063–1066.

Nakayama K, Kim KW and Miyajima A. (2002). *EMBO J.*, **21**, 6174–6184.

Nosaka T, Kawashima T, Misawa K, Ikuta K, Mui AL and Kitamura T. (1999). *EMBO J.*, **18**, 4754–4765.

Nyormoi O and Bar-Eli M. (2003). *Clin. Exp. Metastasis*, **20**, 251–263.

Ogihara H, Morii E, Kim DK, Oboki K and Kitamura Y. (2001). *Blood*, **97**, 645–651.

Ong EK, Griffith IJ, Knox RB and Singh MB. (1993). *Gene*, **134**, 235–240.

Sasaki A, Inagaki-Ohara K, Yoshida T, Yamanaka A, Sasaki M, Yasukawa H, Koromilas AE and Yoshimura A. (2003). *J. Biol. Chem.*, **278**, 2432–2436.

Sato M, Morii E, Takebayashi-Suzuki K, Yasui N, Ochi T, Kitamura Y and Nomura S. (1999). *Biochem. Biophys. Res. Commun.*, **254**, 384–387.

Shibahara S, Takeda K, Yasumoto K, Udono T, Watanabe K, Saito H and Takahashi K. (2001). *J. Invest. Dermatol. Symp. Proc.*, **6**, 99–104.

Shibuya H, Kohu K, Yamada K, Barsoumian EL, Perlmutter RM and Taniguchi T. (1994). *Mol. Cell. Biol.*, **14**, 5812–5819.

Stark GR, Kerr IM, Williams BR, Silverman RH and Schreiber RD. (1998). *Annu. Rev. Biochem.*, **67**, 227–264.

Tachibana M. (1997). *Pigment Cell Res.*, **10**, 25–33.

Tsujimura T, Morii E, Nozaki M, Hashimoto K, Moriyama Y, Takebayashi K, Kondo T, Kanakura Y and Kitamura Y. (1996). *Blood*, **88**, 1225–1233.

Turkson J, Bowman T, Garcia R, Caldenhoven E, De Groot RP and Jove R. (1998). *Mol. Cell. Biol.*, **18**, 2545–2552.

Udono T, Yasumoto K, Takeda K, Amae S, Watanabe K, Saito H, Fuse N, Tachibana M, Takahashi K, Tamai M and Shibahara S. (2000). *Biochim. Biophys. Acta*, **1491**, 205–219.

Ui M, Mizutani T, Takada M, Arai T, Ito T, Murakami M, Koike C, Watanabe T, Yoshimatsu K and Iba H. (2000). *Biochem. Biophys. Res. Commun.*, **278**, 97–105.

Vachtenheim J, Novotna H and Ghanem G. (2001). *J. Invest. Dermatol.*, **117**, 1505–1511.

Yasukawa H, Misawa H, Sakamoto H, Masuhara M, Sasaki A, Wakioka T, Ohtsuka S, Imaizumi T, Matsuda T, Ihle JN and Yoshimura A. (1999). *EMBO J.*, **18**, 1309–1320.

Yoshida T, Hanada T, Tokuhisa T, Kosai K, Sata M, Kohara M and Yoshimura A. (2002). *J. Exp. Med.*, **196**, 641–653.

Yu CL, Meyer DJ, Campbell GS, Larner AC, Carter-Su C, Schwartz J and Jove R. (1995). *Science*, **269**, 81–83.

Zanocco-Marani T, Bateman A, Romano G, Valentinis B, He ZH and Baserga R. (1999). *Cancer Res.*, **59**, 5331–5340.

nature medicine

G-CSF prevents cardiac remodeling after myocardial infarction by activating the Jak-Stat pathway in cardiomyocytes

Mutsuo Harada[1,4], Yingjie Qin[1,4], Hiroyuki Takano[1,4], Tohru Minamino[1,4], Yunzeng Zou[1], Haruhiro Toko[1], Masashi Ohtsuka[1], Katsuhisa Matsuura[1], Masanori Sano[1], Jun-ichiro Nishi[1], Koji Iwanaga[1], Hiroshi Akazawa[1], Takeshige Kunieda[1], Weidong Zhu[1], Hiroshi Hasegawa[1], Keita Kunisada[2], Toshio Nagai[1], Haruaki Nakaya[3], Keiko Yamauchi-Takihara[2] & Issei Komuro[1]

Granulocyte colony-stimulating factor (G-CSF) was reported to induce myocardial regeneration by promoting mobilization of bone marrow stem cells to the injured heart after myocardial infarction, but the precise mechanisms of the beneficial effects of G-CSF are not fully understood. Here we show that G-CSF acts directly on cardiomyocytes and promotes their survival after myocardial infarction. G-CSF receptor was expressed on cardiomyocytes and G-CSF activated the Jak/Stat pathway in cardiomyocytes. The G-CSF treatment did not affect initial infarct size at 3 d but improved cardiac function as early as 1 week after myocardial infarction. Moreover, the beneficial effects of G-CSF on cardiac function were reduced by delayed start of the treatment. G-CSF induced antiapoptotic proteins and inhibited apoptotic death of cardiomyocytes in the infarcted hearts. G-CSF also reduced apoptosis of endothelial cells and increased vascularization in the infarcted hearts, further protecting against ischemic injury. All these effects of G-CSF on infarcted hearts were abolished by overexpression of a dominant-negative mutant Stat3 protein in cardiomyocytes. These results suggest that G-CSF promotes survival of cardiac myocytes and prevents left ventricular remodeling after myocardial infarction through the functional communication between cardiomyocytes and noncardiomyocytes.

Myocardial infarction is the most common cause of cardiac morbidity and mortality in many countries, and left ventricular remodeling after myocardial infarction is important because it causes progression to heart failure. Several cytokines including G-CSF, erythropoietin and leukemia inhibitory factor have beneficial effects on cardiac remodeling after myocardial infarction[1–5]. In particular, G-CSF markedly improves cardiac function and reduce mortality after myocardial infarction in mice, possibly by regeneration of myocardium and angiogenesis[1,2,6–8]. G-CSF is known to have various functions such as induction of proliferation, survival and differentiation of hematopoietic cells, as well as mobilization of bone marrow cells[9–11]. Although it was reported that bone marrow cells could differentiate into cardiomyocytes and vascular cells, thereby contributing to regeneration of myocardium and angiogenesis in ischemic hearts[12–15], accumulating evidence has questioned these previous reports[16–18]. In this study, we examined the molecular mechanisms of how G-CSF prevents left ventricular remodeling after myocardial infarction.

RESULTS

G-CSF directly acts on cultured cardiomyocytes

G-CSF receptor (G-CSFR, encoded by *CSF3R*) has been reported to be expressed only on blood cells such as myeloid leukemic cells, leukemic cell lines, mature neutrophils, platelets, monocytes and some lymphoid cell lines[9]. To test whether G-CSFR is expressed on mouse cardiomyocytes, we performed a reverse transcription–polymerase chain reaction (RT-PCR) experiment by using specific primers for mouse *Csf3r*. We detected expression of the *Csf3r* gene in the adult mouse heart and cultured neonatal cardiomyocytes (**Fig. 1a**). We next examined expression of G-CSFR protein in cultured cardiomyocytes of neonatal rats by immunocytochemistry. Similar to the previously reported expression pattern of G-CSFR in living cells[19], the immunoreactivity for G-CSFR was localized to the cytoplasm and cell membrane under steady-state conditions in cardiomyocytes (**Fig. 1b**). This immunoreactivity disappeared when the antibody specific for G-CSFR was omitted, validating its specificity (**Fig. 1b**). In addition to cardiomyocytes, we also detected expression of G-CSFR on cardiac fibroblasts by immunocytochemistry (see **Supplementary Fig. 1** online) and RT-PCR (**Supplementary Fig. 2** online).

The binding of G-CSF to its receptor has been reported to evoke signal transduction by activating the receptor-associated Janus family tyrosine kinases (JAK) and signal transducer and activator of transcription (STAT) proteins in hematopoietic cells[9,10]. In particular, STAT3

[1]Department of Cardiovascular Science and Medicine, Chiba University Graduate School of Medicine, 1-8-1 Inohana, Chuo-ku, Chiba 260-8670, Japan. [2]Department of Molecular Medicine, Osaka University Medical School, Osaka University, 2-2 Yamadaoka, Suita, Osaka 565-0871, Japan. [3]Department of Pharmacology, Chiba University Graduate School of Medicine, 1-8-1 Inohana, Chuo-ku, Chiba 260-8670, Japan. [4]These authors contributed equally to this work. Correspondence should be addressed to I.K. (komuro-tky@umin.ac.jp).

Published online 20 February 2005; doi:10.1038/nm1199

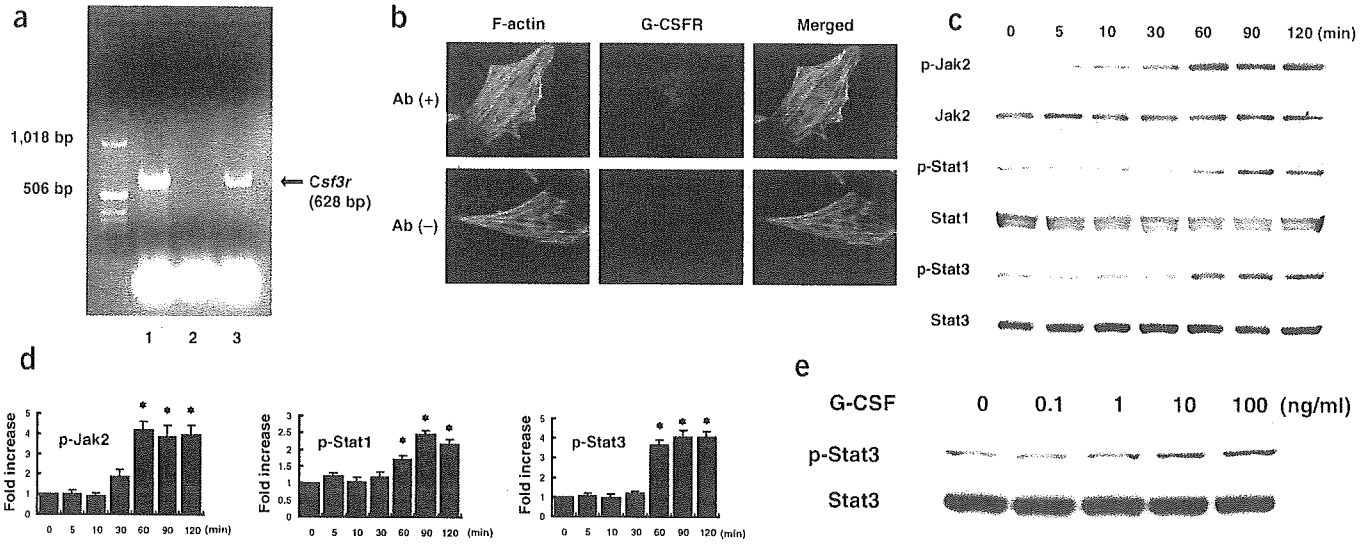

Figure 1 Expression of G-CSFR and the G-CSF-evoked signal transduction in cultured cardiomyocytes. (**a**) RT-PCR for mouse *Csf3r*. Expression of *Csf3r* was detected in the adult mouse heart (lane 1) and cultured cardiomyocytes of neonatal mice (lane 3). In lane 2, reverse transcription products were omitted to exclude the possibility of false-positive results from contamination. (**b**) Immunocytochemical staining for G-CSFR. Cardiomyocytes from neonatal rats were incubated with antibody to G-CSFR (red) and phalloidin (green) (upper panel). In the absence of antibody to G-CSFR, no signal was detected (lower panel). Original magnification, ×1,000. (**c**) G-CSF induces phosphorylation of Jak2, Stat1 and Stat3 in a time-dependent manner in cultured cardiomyocytes. (**d**) Quantification of Jak2, Stat1 and Stat3 activation by G-CSF stimulation as compared with control (time = 0). $^{*}P < 0.05$ versus control ($n = 3$). (**e**) G-CSF induces phosphorylation and activation of Stat3 in a dose-dependent manner in cultured cardiomyocytes.

has been reported to contribute to G-CSF-induced myeloid differentiation and survival[20,21]. We therefore examined whether G-CSF activates the Jak-Stat signaling pathway in cultured cardiomyocytes. G-CSF (100 ng/ml) significantly induced phosphorylation and activation of Jak2 and Stat3, and to a lesser extent, Stat1 but not Jak1, Tyk2 or Stat5 in a dose-dependent manner (**Fig. 1c–e** and data not shown), suggesting that G-CSFR on cardiomyocytes is functional.

We next examined whether G-CSF confers direct protective effects on cardiomyocytes as it prevents hematopoietic cells from apoptotic death[21]. We exposed cardiomyocytes to 0.1 mM H_2O_2 in the absence or presence of G-CSF and examined cardiomyocyte apoptosis by staining with annexin V[22,23]. Pretreatment with G-CSF significantly reduced the number of H_2O_2-induced annexin V–positive cells compared with cells that were not given the G-CSF pretreatment

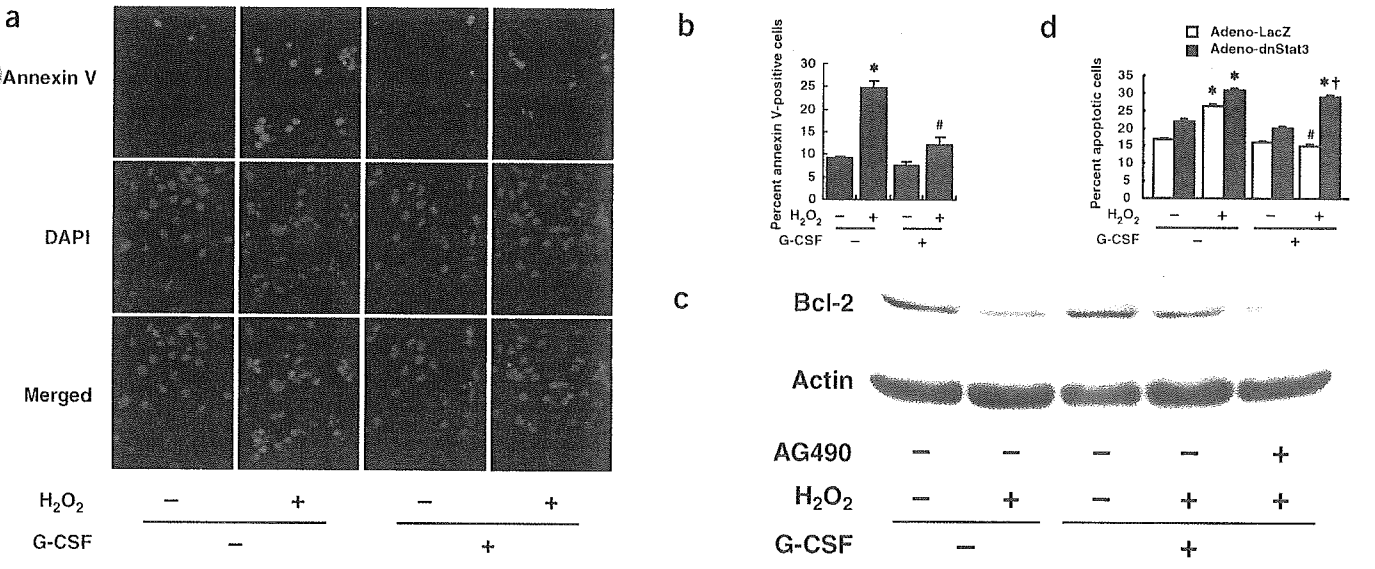

Figure 2 Suppression of H_2O_2-induced cardiomyocyte apoptosis by G-CSF. (**a**) Detection of apoptosis by Cy3-labeled annexin V. Red fluorescence shows apoptotic cardiomyocytes stained with Cy3-labeled annexin V. Nuclei were counterstained with DAPI staining (blue). Original magnification, ×400. (**b**) Quantitative analysis of apoptotic cells. The vertical axis indicates the ratio of the annexin V–positive cell number relative to that of DAPI-positive nuclei. $^{*}P < 0.01$ versus nontreated cells, $^{\#}P < 0.05$ versus H_2O_2-treated cells without G-CSF ($n = 3$). (**c**) G-CSF prevents H_2O_2-induced downregulation of Bcl-2 expression ($n = 3$). (**d**) Inhibition of antiapoptotic effects of G-CSF by Adeno-dnStat3. Bar graphs represent quantitative analysis of the apoptotic cell number relative to the total cell number. $^{*}P < 0.001$ versus H_2O_2 (–)/G-CSF (–), $^{\#}P < 0.001$ versus H_2O_2 (+)/G-CSF (–), $^{\dagger}P < 0.001$ versus H_2O_2 (+)/G-CSF (+)/Adeno-LacZ ($n = 3$).

(**Fig. 2a,b**). To investigate the molecular mechanism of how G-CSF exerts an antiapoptotic effect on cultured cardiomyocytes, we examined expression of the Bcl-2 protein family, known target molecules of the Jak-Stat pathway[24], by western blot analysis. Expression levels of antiapoptotic proteins such as Bcl-2 and Bcl-xL were lower when cardiomyocytes were subjected to H_2O_2 (**Fig. 2c** and data not shown), and this reduction was considerably inhibited by G-CSF pretreatment (**Fig. 2c**). AG490, an inhibitor of Jak2, abolished G-CSF-induced Bcl-2 expression (**Fig. 2c**) but did not affect its basal levels (**Supplementary Fig. 3** online), suggesting a crucial role of the Jak-Stat pathway in inducing survival of cardiomyocytes by G-CSF. To further elucidate the involvement of the Jak-Stat pathway in the protective effects of G-CSF on cardiomyocytes, we transduced cultured cardiomyocytes with adenovirus encoding dominant-negative Stat3 (Adeno-dnStat3). G-CSF treatment significantly reduced apoptosis induced by H_2O_2 in Adeno-LacZ-infected cardiomyocytes (**Fig. 2d**). This effect was abolished by introduction of Adeno-dnStat3 (**Fig. 2d**), suggesting that Stat3 mediates the protective effects of G-CSF on H_2O_2-induced cardiomyocyte apoptosis.

Effects of G-CSF on cardiac function after myocardial infarction

Consistent with the *in vitro* data, G-CSF enhanced activation of Stat3 in the infarcted heart (**Fig. 3a**). Notably, the levels of G-CSFR were markedly increased after myocardial infarction in cardiomyocytes (**Supplementary Fig. 4** online), which may enhance the effects of G-CSF on the infarcted heart. To elucidate the role of G-CSF-induced Stat3 activation in cardiac remodeling, we produced myocardial infarction in transgenic mice which express dominant-negative Stat3 in cardiomyocytes under the control of the α-myosin heavy chain promoter (dnStat3-Tg). Administration of G-CSF was started at the time of coronary artery ligation (day 0) until day 4 in transgenic mice; we termed this group Tg-G mice. A control group of dnStat3-Tg mice given myocardial infarction received saline (Tg-cont) instead of G-CSF. We also included two groups of wild-type mice given myocardial infarction treated with G-CSF (Wt-G) or saline (Wt-cont). At 2 weeks after myocardial infarction, we assessed the morphology by histological analysis and measured cardiac function by echocardiography and catheterization analysis. The infarct area was significantly smaller in the Wt-G group than the Wt-cont group (**Fig. 3b**). The Wt-G group also showed less left ventricular end-diastolic dimension (LVEDD) and better fractional shortening as assessed by echocardiography, and lower end-diastolic pressure (LVEDP) and better $+dp/dt$ and $-dp/dt$ as assessed by cardiac catheterization compared with Wt-cont (**Fig. 3c**). The beneficial effects of G-CSF on cardiac function were dose dependent and were significantly reduced by delayed start of the treatment (**Fig. 3d,e** and **Supplementary Fig. 5** online). Moreover, its favorable effects on cardiac function became evident within 1 week after the treatment (**Fig. 3f**). Disruption of the Stat3 signaling pathway in cardiomyocytes abolished the protective effects of G-CSF. There was no significant difference in LVEDD, fractional shortening, LVEDP, $+dp/dt$ and $-dp/dt$ between Tg-G and Tg-cont (**Fig. 3c**). We obtained similar results from infarcted female hearts (**Fig. 3g**). These results suggest that G-CSF protects the heart after myocardial infarction at least in part by directly activating Stat3 in cardiomyocytes, which is a gender-independent effect. We have previously shown that treatment with G-CSF significantly ($P < 0.05$) decreased myocardial infarction–related mortality of wild-type mice[2]. In contrast, there were no significant differences in mortality between G-CSF-treated and saline-treated dnStat3-Tg mice (data not shown).

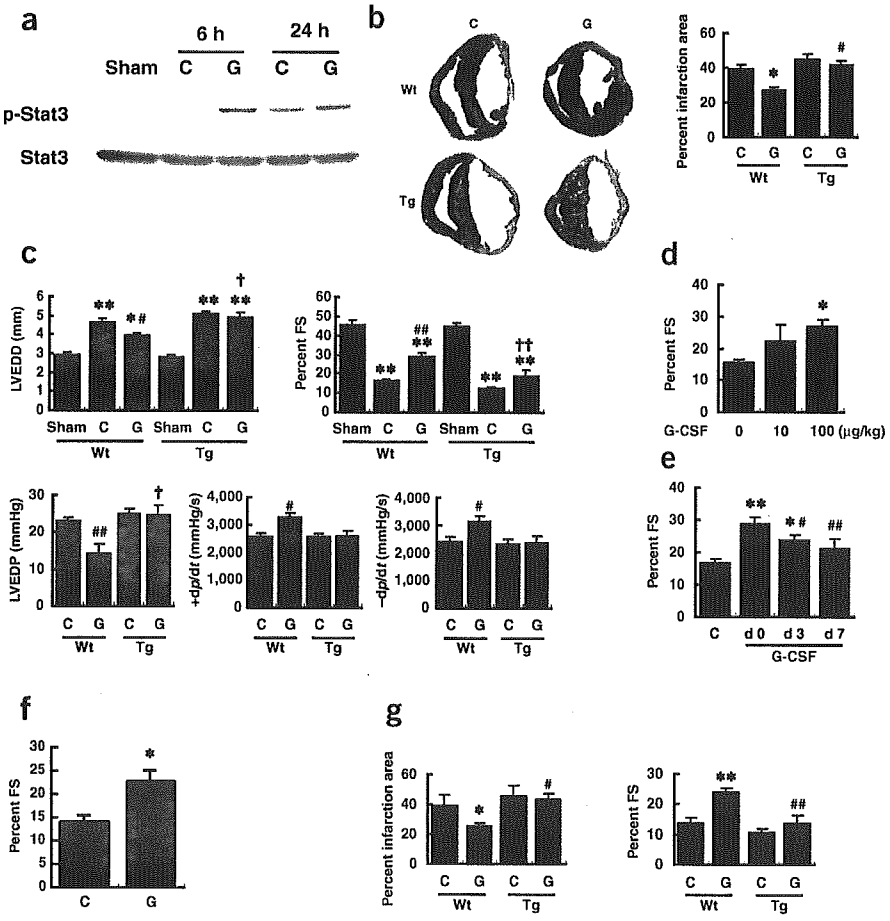

Figure 3 Effects of G-CSF on cardiac function after myocardial infarction. (**a**) Stat3 activation in the infarcted hearts. We operated on wild-type mice to induce myocardial infarction and treated them with G-CSF (G) or saline (C). (**b**) Masson trichrome staining of wild-type (Wt) and dnStat3-Tg (Tg) hearts. $^{*}P < 0.001$ versus Wt-cont, $^{\#}P < 0.001$ versus Wt-G ($n = 11$–15). (**c**) G-CSF treatment preserves cardiac function after myocardial infarction. $^{*}P < 0.01$, $^{**}P < 0.001$ versus sham; $^{\#}P < 0.05$, $^{\#\#}P < 0.001$ versus Wt-cont; $^{\dagger}P < 0.01$, $^{\dagger\dagger}P < 0.001$ versus Wt-G ($n = 10$–15 for echocardiography and $n = 5$ for catheterization analysis). (**d**) Dose-dependent effects of G-CSF. FS, fractional shortening. $^{*}P < 0.01$ versus saline-treated mice (G-CSF = 0)($n = 12$–14). (**e**) Wild-type mice were operated to induce myocardial infarction and G-CSF treatment (100 μg/kg/d) was started from the indicated day for 5 d. $^{*}P < 0.05$, $^{**}P < 0.001$ versus saline-treated mice (C); $^{\#}P < 0.05$, $^{\#\#}P < 0.01$ versus mice treated at day 0 (d 0) ($n = 11$–12). (**f**) Effects of G-CSF on cardiac function at 1 week. $^{*}P < 0.05$ versus control ($n = 3$). (**g**) Effects of G-CSF on cardiac function of female mice. $^{*}P < 0.05$, $^{**}P < 0.001$ versus Wt-cont; $^{\#}P < 0.05$, $^{\#\#}P < 0.005$ versus Wt-G ($n = 4$–5).

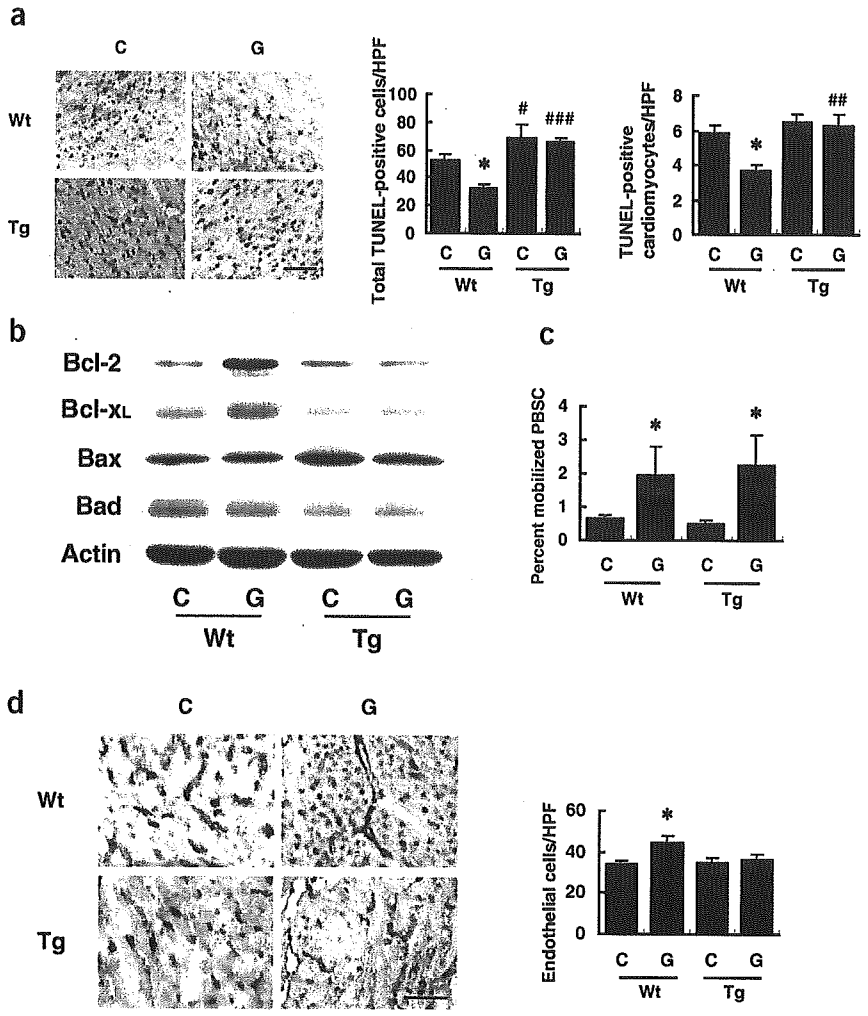

Figure 4 Mechanisms of the protective effects of G-CSF. (**a**) TUNEL staining (brown nuclei) in the infarcted hearts. The graphs show quantitative analyses for total TUNEL-positive cells (left graph) and TUNEL-positive cardiomyocytes (right graph) in infarcted hearts. $^{*}P < 0.01$ versus Wt-cont; $^{\#}P < 0.05$, $^{\#\#}P < 0.005$, $^{\#\#\#}P < 0.001$ versus wild-type mice with the same treatment ($n = 5$–7). Scale bar, 100 μm. (**b**) Infarcted hearts treated with G-CSF (G) or saline (C) were analyzed for expression of Bcl-2, Bcl-xL, Bax and Bad by western blotting ($n = 3$). (**c**) Mobilization of hematopoietic stem cells into peripheral blood (PBSC). $^{*}P < 0.05$ versus saline-treated mice ($n = 4$). (**d**) Capillary endothelial cells were identified by immunohistochemical staining with anti-PECAM antibody in the border zone of the infarcted hearts. Scale bar, 100 μm. The number of endothelial cells was counted and shown in the graph ($n = 6$–8). $^{*}P < 0.05$.

Mechanisms of the protective effects of G-CSF

Our *in vitro* results suggest that the protective effects of G-CSF on cardiac remodeling after myocardial infarction can be attributed in part to reduction of cardiomyocyte apoptosis. To determine whether the Stat3 pathway in cardiomyocytes mediates the antiapoptotic effects of G-CSF on the ischemic myocardium, we carried out TUNEL labeling of left ventricular sections 24 h after myocardial infarction in wild-type mice and dnStat3-Tg mice. Although the number of TUNEL-positive cells was significantly less in the Wt-G group than the Wt-cont group, G-CSF treatment had no effect on cardiomyocyte apoptosis in dnStat3-Tg mice (**Fig. 4a**). The effects of G-CSF on apoptosis after myocardial infarction were also attenuated when mice were treated with AG490 (**Supplementary Fig. 6** online). Myocardial infarction–related apoptosis was significantly increased in the Tg-cont group and AG490-treated wild-type mice compared with Wt-cont mice (**Fig. 4a** and **Supplementary Fig. 6** online), suggesting that endogenous activation of Stat3 has a protective role in the infarcted heart, as reported previously[25]. It is noteworthy that G-CSF treatment inhibited apoptosis of noncardiomyocytes including endothelial cells and that this inhibition was abolished in dnStat3-Tg mice (**Fig. 4a** and data not shown). To investigate the underlying molecular mechanism of the antiapoptotic effects of G-CSF *in vivo*, we examined expression of the Bcl-2 protein family by western blot analysis. Consistent with our *in vitro* results, expression of antiapoptotic proteins such as Bcl-2 and Bcl-xL was significantly increased in the Wt-G group at 24 h after myocardial infarction compared with the Wt-cont group, whereas expression of the proapoptotic proteins Bax and Bad was not affected by the treatment (**Fig. 4b**). In contrast, expression levels of antiapoptotic proteins were not increased by G-CSF in the Tg-G group (**Fig. 4b**). Immunohistochemical analysis also showed increased expression of Bcl-2 in the infarcted heart of the Wt-G group but not of the Tg-G group (**Supplementary Fig. 7** online).

To determine the effects of G-CSF on mobilization of stem cells, we counted the number of cells positive for both Sca-1 and c-kit in peripheral blood samples from mice treated with G-CSF or saline. The G-CSF treatment similarly increased the number of double-positive cells in wild-type mice and dnStat3-Tg mice (**Fig. 4c**). To examine the impact of G-CSF on cardiac homing of bone marrow cells, we transplanted bone marrow cells derived from GFP transgenic mice into wild-type and dnStat3-Tg mice, produced myocardial infarction and treated with G-CSF or saline. FACS analysis showed that G-CSF did not increase cardiac homing of bone marrow cells in wild-type and dnStat3-Tg mice (**Supplementary Fig. 8** online). We have shown that cardiac stem cells, which are able to differentiate into cardiomyocytes, exist in Sca-1-positive populations in the adult myocardium[26]. But G-CSF treatment did not affect the number of Sca-1-positive cells in the infarcted hearts of wild-type or dnStat3-Tg mice (**Supplementary Fig. 9** online). Thus, it is unlikely that G-CSF exerts its beneficial effects through expansion of cardiac stem cells. To determine the effects of G-CSF on proliferation of cardiomyocytes, we carried out immunostaining for Ki67, a marker for cell cycling, in conjunction with a labeling for troponin T. The number of Ki67-positive cardiomyocytes was increased in the infarcted hearts of wild-type mice and dnStat3-Tg mice compared with sham-operated mice (**Supplementary Fig. 10** online). But G-CSF did not alter the number of Ki67-positive cardiomyocytes in wild-type or dnStat3-Tg mice, suggesting that G-CSF does not induce proliferation of cardiomyocytes (**Supplementary Fig. 10** online). The number of Ki67-positive cardiomyocytes was less in infarcted hearts of dnStat3-Tg mice than in those of wild-type mice, suggesting that endogenous Stat3 activity is required

for myocardial regeneration after myocardial infarction and that activation of Stat3 by G-CSF is not sufficient for cardiomyocytes to enter the cell cycle in infarcted hearts of wild-type mice (**Supplementary Fig. 10** online). In contrast, G-CSF treatment significantly increased the number of endothelial cells in the border zone of the infarcted hearts (**Fig. 4d**). This increase was attenuated in dnStat3-Tg mice, indicating that the increased vascularity is mediated by Stat3 activity in cardiomyocytes and may partially account for the beneficial effects of G-CSF on the infarcted hearts. Taken together with the result that G-CSF-induced inhibition of noncardiomyocyte apoptosis was also mediated by the Stat3 signaling pathway in cardiomyocytes (**Fig. 4a**), these findings imply that communication between cardiomyocytes and noncardiomyocytes regulates each others' survival.

To further test whether G-CSF acts directly on the heart, we examined the effects of G-CSF treatment on cardiac function after ischemia-reperfusion injury in a Langendorff perfusion model. The isolated hearts underwent 30 min total ischemia followed by 120 min reperfusion with the perfusate containing G-CSF (300 ng/ml) or vehicle, and left ventricular developed pressure (LVDP, measured as the difference between systolic and diastolic pressures of the left ventricle) and LVEDP were measured. There were no significant differences in basal hemodynamic parameters including heart rate, left ventricular pressure, LVEDP and positive and negative d*p*/d*t*, between the control group and G-CSF group (**Table 1**). After reperfusion, however, G-CSF-treated hearts started to beat earlier than those of the control group (**Fig. 5a**). At 120 min after reperfusion, contractile function (LVDP) of G-CSF-treated hearts was significantly better than that of control hearts (**Fig. 5a**). Likewise, diastolic function (LVEDP) of G-CSF-treated hearts was better than that of control hearts (**Fig. 5a**). After ischemia-reperfusion, there was more viable myocardium (red lesion) in G-CSF-treated hearts than control hearts (**Fig. 5b**). The size of the infarct (white lesion) was significantly smaller in G-CSF-treated hearts than in control hearts (**Fig. 5b**).

Table 1 Basal hemodynamic parameters

	Control ($n = 7$)	G-CSF ($n = 7$)
HR (b.p.m.)	326 ± 34	334 ± 24
LVP (mmHg)	121.8 ± 24	117.3 ± 32
LVEDP (mmHg)	4.3 ± 1.3	4.5 ± 1.6
+d*p*/d*t* (mmHg/s)	7,554 ± 643	7,657 ± 377
−d*p*/d*t* (mmHg/s)	6,504 ± 638	6,670 ± 602

HR, heart rate; b.p.m., beats per minute; LVP, left ventricular pressure; LVEDP, left ventricular end-diastolic pressure; +d*p*/d*t* and −d*p*/d*t*, positive and negative first derivatives for maximal rates of left ventricular pressure development.

DISCUSSION

In the present study, G-CSFR was found to be expressed on cardiomyocytes and cardiac fibroblasts, and G-CSF activated Jak2 and the downstream signaling molecule Stat3 in cultured cardiomyocytes. Treatment with G-CSF protected cultured cardiomyocytes from apoptotic cell death possibly through upregulation of Bcl-2 and Bcl-xL expression, suggesting that G-CSF has direct protective effects on cardiomyocytes through G-CSFR and the Jak-Stat pathway. This idea is further supported by the *in vivo* experiments. G-CSF enhanced Stat3 activity and increased expression of Bcl-2 and Bcl-xL in the infarcted heart where G-CSFR was markedly upregulated, thereby preventing cardiomyocyte apoptosis and cardiac dysfunction. These effects of G-CSF were abolished when Stat3 activation was disrupted in cardiomyocytes, suggesting that a direct action of G-CSF on cardiomyocytes has a crucial role in preventing left ventricular remodeling after myocardial infarction. Because noncardiomyocytes also expressed G-CSFR, the possibility exists that activation of G-CSF receptors on these cells modulates the beneficial effects of G-CSF on infarcted hearts.

The mobilization of bone marrow stem cells (BMSC) to the myocardium has been considered to be the main mechanism by which G-CSF ameliorates cardiac remodeling after myocardial infarction[1,6–8]. In this study, we showed that G-CSF reduces apoptotic cell death and effectively protects the infarcted heart, which is dependent on its direct action on cardiomyocytes through the Stat3 pathway. This antiapoptotic mechanism seems to be more important than induction of BMSC mobilization, because disruption of

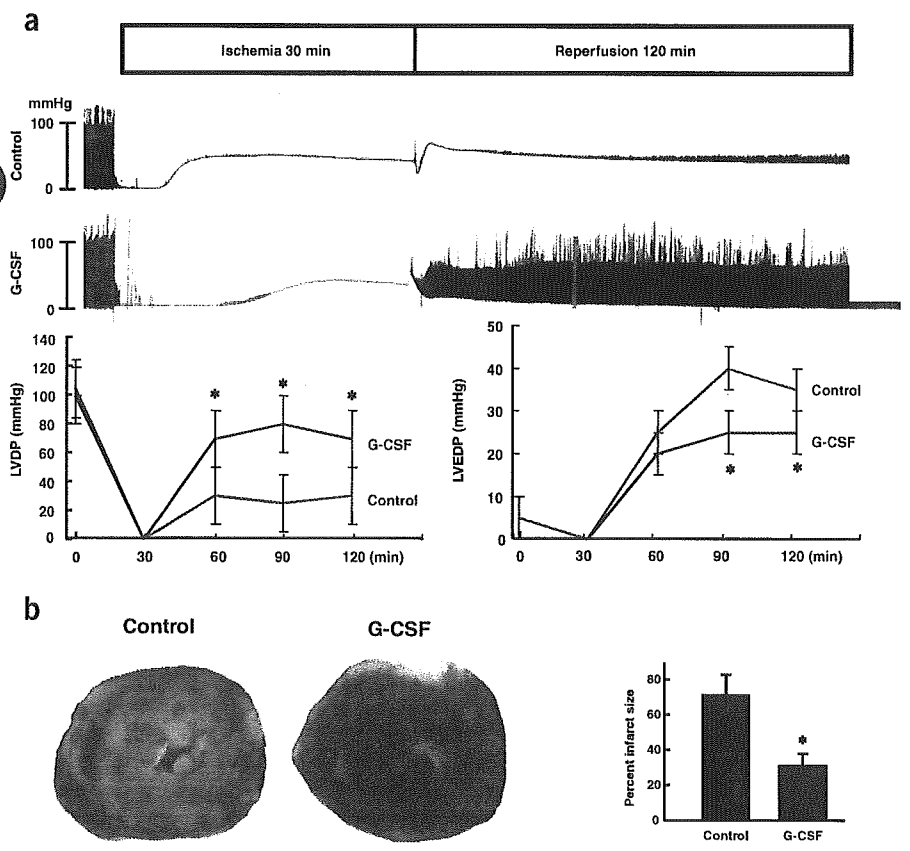

Figure 5 Direct effects of G-CSF on cardiac function after ischemia-reperfusion injury. (**a**) Representative left ventricular pressure records of control and G-CSF-treated hearts are shown (upper panel). The graphs show changes in LVDP (left) and LVEDP (right) during ischemia-reperfusion. *$P < 0.05$ versus control hearts ($n = 7$). (**b**) The photographs show representative TTC staining of control hearts (Control) and G-CSF-treated hearts (G-CSF) after ischemia-reperfusion. The graph indicates myocardial infarct sizes for control hearts (Control) and G-CSF-treated hearts (G-CSF). Infarct sizes were calculated as described in **Supplementary Methods** online. *$P < 0.05$ versus control hearts ($n = 7$).

this pathway by expressing dnStat3 in cardiomyocytes almost abolished the protective effects of G-CSF on cardiac remodeling after myocardial infarction. In addition, there was no difference in the effects of G-CSF on mobilization and cardiac homing of bone marrow cells, expansion of cardiac stem cells, and proliferation of cardiomyocytes between wild-type and dnStat3-Tg mice. The beneficial effects of G-CSF and stem cell factor on the infarcted heart has been described, but no evidence indicating that G-CSF induced cardiac homing of bone marrow cells in the infarcted heart has been shown[1]. In this study, we found favorable effects of G-CSF on the infarcted heart as early as 1 week after the treatment even though cardiac homing of bone marrow cells was not increased. Thus, we conclude that increased cardiac homing of bone marrow cells cannot account for improved function of the infarcted heart after G-CSF treatment.

The JAK-STAT pathway has been shown to induce various angiogenic factors besides antiapoptotic proteins[20,21]. The number of endothelial cells in the border zone was increased by G-CSF through Stat3 activation in cardiomyocytes. Consistent with this, we noted that G-CSF induces cardiac expression of angiogenic factors *in vitro* and *in vivo*, which appears to be mediated by cardiac Stat3 activation (M.H., Y.Q., H.T., T.M. & I.K., unpublished data). Moreover, we observed that the majority of apoptotic cells in the infarcted hearts was endothelial cells and that endothelial apoptosis was significantly inhibited by G-CSF treatment in wild-type mice but not in dnStat3-Tg mice (**Fig. 4a** and M.H., T.M. & I.K., unpublished data). Thus, activation of this pathway in cardiomyocytes by G-CSF may also promote angiogenesis and protect against endothelial apoptosis by producing angiogenic factors, resulting in the further prevention of cell death of cardiomyocytes and cardiac remodeling after myocardial infarction. The results in this study provide new mechanistic insights of the G-CSF therapy on infarcted hearts.

METHODS

For further details, please see **Supplementary Methods** online.

Cell culture. Cardiomyocytes prepared from ventricles of 1-d-old Wistar rats[27] were plated onto 60-mm plastic culture dishes at a concentration of 1×10^5 cells/cm^2 and cultured in Dulbecco modified Eagle medium (DMEM) supplemented with 10% fetal bovine serum (FBS) at 37 °C in a mixture of 95% air and 5% CO_2. The culture medium was changed to serum-free DMEM 24 h before stimulation. Generation and infection of recombinant adenovirus were performed as described[28].

Percoll enrichment of adult mouse cardiomyocytes and noncardiomyocytes. Adult mouse cardiomyocytes were prepared from 10-week-old C57BL/6 male mice according to the Alliance for Cellular Signaling protocol. We also prepared cardiomyocytes and noncardiomyocytes from myocardial infarction-operated or sham-operated C57BL/6 male mice. After digestion, cells were dissociated, resuspended in differentiation medium and loaded onto a discontinuous Percoll gradient. Cardiomyocytes or noncardiomyocytes were separately collected as described previously[29] and subsequently washed with 1 × phosphate-buffered saline for RT-PCR.

RNA extraction and RT-PCR analysis. Total RNA from adult mice cardiomyocytes was isolated by the guanidinium thiocyanate-phenol chloroform method. A total of 4 μg RNA was transcribed with MMLV reverse transcriptase and random hexamers. The cDNA was amplified using a mouse *Csf3r* exon 15 forward primer (5′-GTACTCTTGTCCACTACCTGT -3′) and an exon 17 reverse primer (5′-CAAGATACAAGGACCCCCAA -3′). We performed PCR under the following conditions: an initial denaturation at 94 °C for 2 min followed by a cycle of denaturation at 94 °C for 1 min, annealing at 58 °C for 1 min and extension at 72 °C for 1 min. We subjected samples to 40 cycles followed by a final extension at 72 °C for 3 min. The products were analyzed on a 1.5% ethidium bromide stained agarose gel.

Immunocytochemistry. Cardiomyocytes or noncardiomyocytes of neonatal rats cultured on glass cover slips were incubated with or without the antibody to G-CSFR (Santa Cruz Biotechnology) for 1 h, followed by incubation with Cy3-labeled secondary antibodies. After washing, we double-stained the cells with fluorescent phalloidin (Molecular Probes) for 1 h at room temperature.

Western blots. Western blot analysis was performed as described[5]. We probed the membranes with antibodies to phospho-Jak2, phospho-Stat3 (Cell Signaling), phospho-Jak1, phospho-Tyk2, phospho-Stat1, phospho-Stat5, anti-Jak1, Jak2, Tyk2, Stat1, Stat3, Stat5, Bcl-2, Bax, G-CSFR (Santa Cruz Biotechnology), Bcl-xL, Bad (Transduction Laboratories) or actin (Sigma-Aldrich). We used the ECL system (Amersham Biosciences Corp) for detection.

Animals and surgical procedures. Generation and genotyping of dnStat3-Tg mice have been previously described[28]. All mice used in this study were 8–10-week-old males, unless indicated. All experimental procedures were performed according to the guidelines established by Chiba University for experiments in animals and all protocols were approved by our institutional review board. We anesthetized mice by intraperitoneally injecting a mixture of 100 mg/kg ketamine and 5 mg/kg xylazine. Myocardial infarction was produced by ligation of the left anterior descending artery. We operated on dnStat3-Tg mice to induce myocardial infarction and randomly divided them into two groups, the G-CSF-treated group (10–100 μg/kg/d subcutaneously for 5 d consecutively, Kyowa Hakko Kogyo Co.) and the saline-treated group. We operated on nontransgenic mice as control groups using the same procedures and divided them into a G-CSF-treated group and a saline-treated group. Some mice were randomly chosen to be analyzed for initial area at risk by injection of Evans blue dye after producing myocardial infarction. There was no difference in initial area sizes at risk between saline-treated control and G-CSF-treated mice ($n = 5$; **Supplementary Fig. 11** online). We also determined initial infarct size by triphenyltetrazolium chloride staining on day 3. There was no significant difference in initial infarct size between saline-treated control and G-CSF-treated mice ($n = 5$; **Supplementary Fig. 12** online).

Echocardiography and catheterization. Transthoracic echocardiography was performed with an Agilent Sonos 4500 (Agilent Technology Co.) provided with an 11-MHz imaging transducer. For catheterization analysis, the right carotid artery was cannulated under anesthesia by the micro pressure transducers with an outer diameter of 0.42 mm (Samba 3000; Samba Sensors AB), which was then advanced into the left ventricle. Pressure signals were recorded using a MacLab 3.6/s data acquisition system (AD Instruments) with a sampling rate of 2,000 Hz. Mice were anesthetized as described above, and heart rate was kept at approximately 270–300 beats per minute to minimize data deviation when we measured cardiac function.

Histology. Hearts fixed in 10% formalin were embedded in paraffin, sectioned at 4 μm thickness, and stained with Masson trichrome. The extent of fibrosis was measured in three sections from each heart and the value was expressed as the ratio of Masson trichrome stained area to total left ventricular free wall. For apoptosis analysis, infarcted hearts were frozen in cryomolds, sectioned, and TUNEL labeling was performed according to the manufacturer's protocol (*In Situ* Apoptosis Detection kit; Takara) in combination with immunostainings for appropriate cell markers. Digital photographs were taken at magnification ×400, and 25 random high-power fields (HPF) from each heart sample were chosen and quantified in a blinded manner. We examined vascularization by measuring the number of capillary endothelial cells in light-microscopic sections taken from the border zone of the hearts 2 weeks after myocardial infarction. Capillary endothelial cells were identified by immunohistochemical staining with antibody to platelet endothelial cell adhesion molecule (PECAM; Pharmingen). Ten random microscopic fields in the border zone were examined and the number of endothelial cells was expressed as the number of PECAM-positive cells/HPF (magnification, ×400).

Statistical analysis. Data are shown as mean ± s.e.m. Multiple group comparison was performed by one-way analysis of variance (ANOVA) followed by the Bonferroni procedure for comparison of means. Comparison between two groups were analyzed by the two-tailed Student's *t*-test or two-way ANOVA. Values of $P < 0.05$ were considered statistically significant.

URL. Alliance for Cellular Signaling Procedure Protocols
http://www.signaling-gateway.org/data/cgi-bin/Protocols.cgi?cat=0

Note: Supplementary information is available on the Nature Medicine website.

ACKNOWLEDGMENTS
The authors thank J. Robbins (Children's Hospital Research Foundation, Cincinnati, Ohio) for a fragment of the αMHC gene promoter, M. Tamagawa for the analysis of Langendorff-perfused model, Kirin Brewery Co., Ltd. for their kind gift of G-CSF, and M. Watanabe and E. Fujita for their technical assistance. This work was supported by a Grant-in-Aid for Scientific Research, Developmental Scientific Research, and Scientific Research on Priority Areas from the Ministry of Education, Science, Sports, and Culture and by the Program for Promotion of Fundamental Studies in Health Sciences of the Organization for Drug ADR Relief, R&D Promotion and Product Review of Japan (to I.K.) and Japan Research Foundation for Clinical Pharmacology (to T.M.).

COMPETING INTERESTS STATEMENTS
The authors declare that they have no competing financial interests.

Received 8 September 2004; accepted 19 January 2005
Published online at http://www.nature.com/naturemedicine/

1. Orlic, D. *et al.* Mobilized bone marrow cells repair the infarcted heart, improving function and survival. *Proc. Natl. Acad. Sci. USA* **98**, 10344–10349 (2001).
2. Ohtsuka, M. *et al.* Cytokine therapy prevents left ventricular remodeling and dysfunction after myocardial infarction through neovascularization. *FASEB J.* **18**, 851–853 (2004).
3. Moon, C. *et al.* Erythropoietin reduces myocardial infarction and left ventricular functional decline after coronary artery ligation in rats. *Proc. Natl. Acad. Sci. USA* **100**, 11612–11617 (2003).
4. Parsa, C.J. *et al.* A novel protective effect of erythropoietin in the infarcted heart. *J. Clin. Invest.* **112**, 999–1007 (2003).
5. Zou, Y. *et al.* Leukemia inhibitory factor enhances survival of cardiomyocytes and induces regeneration of myocardium after myocardial infarction. *Circulation* **108**, 748–753 (2003).
6. Minatoguchi, S. *et al.* Acceleration of the healing process and myocardial regeneration may be important as a mechanism of improvement of cardiac function and remodeling by postinfarction granulocyte colony-stimulating factor treatment. *Circulation* **109**, 2572–2580 (2004).
7. Adachi, Y. *et al.* G-CSF treatment increases side population cell infiltration after myocardial infarction in mice. *J. Mol. Cell. Cardiol.* **36**, 707–710 (2004).
8. Kawada, H. *et al.* Nonhematopoietic mesenchymal stem cells can be mobilized and differentiate into cardiomyocytes after myocardial infarction. *Blood* **104**, 3581–3587 (2004).
9. Avalos, B.R. Molecular analysis of the granulocyte colony-stimulating factor receptor. *Blood* **88**, 761–777 (1996).
10. Demetri, G.D. & Griffin, J.D. Granulocyte colony-stimulating factor and its receptor. *Blood* **78**, 2791–808 (1991).
11. Berliner, N. *et al.* Granulocyte colony-stimulating factor induction of normal human bone marrow progenitors results in neutrophil-specific gene expression. *Blood* **85**, 799–803 (1995).
12. Orlic, D. *et al.* Bone marrow cells regenerate infarcted myocardium. *Nature* **410**, 701–705 (2001).
13. Asahara, T. *et al.* Bone marrow origin of endothelial progenitor cells responsible for postnatal vasculogenesis in physiological and pathological neovascularization. *Circ. Res.* **85**, 221–228 (1999).
14. Kocher, A.A. *et al.* Neovascularization of ischemic myocardium by human bone-marrow-derived angioblasts prevents cardiomyocyte apoptosis, reduces remodeling and improves cardiac function. *Nat. Med.* **7**, 430–436 (2001).
15. Jackson, K.A. *et al.* Regeneration of ischemic cardiac muscle and vascular endothelium by adult stem cells. *J. Clin. Invest.* **107**, 1395–1402 (2001).
16. Balsam, L.B. *et al.* Haematopoietic stem cells adopt mature haematopoietic fates in ischaemic myocardium. *Nature* **428**, 668–673 (2004).
17. Murry, C.E. *et al.* Haematopoietic stem cells do not transdifferentiate into cardiac myocytes in myocardial infarcts. *Nature* **428**, 664–668 (2004).
18. Norol, F. *et al.* Influence of mobilized stem cells on myocardial infarct repair in a nonhuman primate model. *Blood* **102**, 4361–4368 (2003).
19. Aarts, L.H., Roovers, O., Ward, A.C. & Touw, I.P. Receptor activation and 2 distinct COOH-terminal motifs control G-CSF receptor distribution and internalization kinetics. *Blood* **103**, 571–579 (2004).
20. Benekli, M., Baer, M.R., Baumann, H. & Wetzler, M. Signal transducer and activator of transcription proteins in leukemias. *Blood* **101**, 2940–2954 (2003).
21. Smithgall, T.E. *et al.* Control of myeloid differentiation and survival by Stats. *Oncogene* **19**, 2612–2618 (2000).
22. Dumont, E.A. *et al.* Cardiomyocyte death induced by myocardial ischemia and reperfusion: measurement with recombinant human annexin-V in a mouse model. *Circulation* **102**, 1564–1568 (2000).
23. van Heerde, W.L. *et al.* Markers of apoptosis in cardiovascular tissues: focus on Annexin V. *Cardiovasc. Res.* **45**, 549–559 (2000).
24. Bromberg, J. Stat proteins and oncogenesis. *J. Clin. Invest.* **109**, 1139–1142 (2002).
25. El-Adawi, H. *et al.* The functional role of the JAK-STAT pathway in post-infarction remodeling. *Cardiovasc. Res.* **57**, 129–138 (2003).
26. Matsuura, K. *et al.* Adult cardiac Sca-1-positive cells differentiate into beating cardiomyocytes. *J. Biol. Chem.* **279**, 11384–11391 (2004).
27. Zou, Y. *et al.* Both Gs and Gi proteins are critically involved in isoproterenol-induced cardiomyocyte hypertrophy. *J. Biol. Chem.* **274**, 9760–9770 (1999).
28. Funamoto, M. *et al.* Signal transducer and activator of transcription 3 is required for glycoprotein 130-mediated induction of vascular endothelial growth factor in cardiac myocytes. *J. Biol. Chem.* **275**, 10561–10566 (2000).
29. Ikeda, K. *et al.* The effects of sarpogrelate on cardiomyocyte hypertrophy. *Life Sci.* **67**, 2991–2996 (2000).

Phosphatidylinositol 3-Kinase–Akt Pathway Plays a Critical Role in Early Cardiomyogenesis by Regulating Canonical Wnt Signaling

Atsuhiko T. Naito, Hiroshi Akazawa, Hiroyuki Takano, Tohru Minamino, Toshio Nagai, Hiroyuki Aburatani, Issei Komuro

Abstract—We have recently reported that activation of phosphatidylinositol 3-kinase (PI3K) plays a critical role in the early stage of cardiomyocyte differentiation of P19CL6 cells. We here examined molecular mechanisms of how PI3K is involved in cardiomyocyte differentiation. DNA chip analysis revealed that expression levels of Wnt-3a were markedly increased and that the Wnt/β-catenin pathway was activated temporally during the early stage of cardiomyocyte differentiation of P19CL6 cells. Activation of the Wnt/β-catenin pathway during this period was required and sufficient for cardiomyocyte differentiation of P19CL6 cells. Inhibition of the PI3K/Akt pathway suppressed the Wnt/β-catenin pathway by activation of glycogen synthase kinase-3β (GSK-3β) and degradation of β-catenin. Suppression of cardiomyocyte differentiation by inhibiting the PI3K/Akt pathway was rescued by forced expression of a nonphosphorylated, constitutively active form of β-catenin. These results suggest that the PI3K pathway regulates cardiomyocyte differentiation through suppressing the GSK-3β activity and maintaining the Wnt/β-catenin activity. (*Circ Res.* 2005;97:144-151.)

Key Words: PI3K ■ Akt ■ Wnt ■ cardiomyocyte differentiation

The heart is the first organ to be formed from mesodermal cells during embryogenesis, and its developmental process consists of multiple steps such as commitment of immature mesodermal cells into cardiac mesodermal cells, subsequent differentiation of cardiac mesodermal cells into cardiomyocytes, and morphogenesis of the chambered heart. The study of cell fate mapping has revealed that the cells committed into cardiac cell fate are delineated in the posterior lateral region of the epiblast of the mouse embryo during the early gastrulation. These progenitor cells migrate through the node and primitive streak to a cranial destination, and start to express cardiac transcription factors such as Nkx-2.5 and GATA-4.[1,2] After gastrulation, these cells move to the anterior lateral part of the embryo and merge at their anterior margins to form cardiac crescent. Then these cells move ventrally and fuse at the midline to create linear heart tube.[3] Advances in molecular biology made it possible to identify many important cardiac transcription factors such as Nkx-2.5, GATA-4, HAND1/2, and MEF2C that serially or synergistically induce the expression of cardiac specific genes and regulate morphogenesis of the developing heart. These genes are also used as a marker for cardiomyocyte differentiation in developing embryos.

Mechanisms of how mesodermal cells are committed to cardiac mesodermal cells, in other words, mechanisms of how expression of these transcription factors are regulated initially, have been largely unknown. Explant cultures of the amphibian and avian embryos revealed that secreted proteins from neighboring endoderm, ectoderm, and the mesoderm itself, play important roles in induction of cardiac transcription factors and differentiation of cardiomyocytes.[4] Among such molecules, bone morphogenetic proteins (BMP) and fibroblast growth factors (FGF) have been reported to induce cardiomyocyte differentiation from noncardiac mesodermal cells.[5,6] However, several recent studies reported that BMP is required for the maintenance but not for the induction of cardiac transcription factors.[7,8] Moreover, FGF expression seems to be downstream of BMP,[6] indicating that molecules other than BMP and FGF are required for initial expression of cardiac transcription factors.

Wnt signaling is involved in the development of many organs of various species.[9] In Drosophila, wingless, a homologue of vertebrate Wnt has been reported to be involved in initial expression of tinman, a Drosophila homologue of Nkx-2.5, through armadillo, a Drosophila homologue of β-catenin, and drives heart development.[10] In vertebrates, however, canonical Wnt pathway, which uses β-catenin as a downstream molecule, has been reported to inhibit cardiomyocyte differentiation from cardiac mesoderm.[11–13] On the

Original received February 7, 2005; revision received June 16, 2005; accepted June 17, 2005.

From the Department of Cardiovascular Science and Medicine (A.T.N., H. Akazawa, H.T., T.M., T.N., I.K.), Chiba University Graduate School of Medicine, Japan; and the Research Center for Advanced Science and Technology (H. Aburatani), University of Tokyo, Japan.

Correspondence to Dr Issei Komuro, Department of Cardiovascular Science and Medicine, Chiba University Graduate School of Medicine, 1-8-1 Inohana, Chuo-ku, Chiba 260-8670, Japan. E-mail komuro-tky@umin.ac.jp

Circulation Research is available at http://circres.ahajournals.org

DOI: 10.1161/01.RES.0000175241.92285.f8

other hand, Pandur and colleagues reported that Wnt-11, which uses noncanonical Wnt pathway independently of β-catenin,[14] was required and sufficient for cardiomyocyte differentiation.[15] These reports collectively suggest that noncanonical Wnt pathway plays a positive role, whereas canonical Wnt pathway plays a negative role in cardiomyocyte differentiation.

In spite of the well-designed studies using explant cultures in amphibian or avian embryos, it is difficult to dissect the role of various factors such as BMP, FGF, and Wnt in the cardiac development through the whole process. Moreover, it is hard to elucidate the mechanism of commitment of mesodermal cells into cardiomyocytes in mammalians because of difficulty in explant culture using mammalian embryo of a very early stage. From this viewpoint, in vitro differentiation system, in particular P19CL6 cells, a clonal derivative of murine teratocarcinoma P19 cells, is a very useful model. We have recently demonstrated that TAK-1 and Smad proteins play critical roles in cardiomyocyte differentiation downstream of BMP receptor.[16,17] More recently, Nakamura et al have reported that canonical Wnt pathway is required for differentiation of P19CL6 cells into cardiomyocytes.[18]

We have recently reported that phosphatidylinositol 3-kinase (PI3K) pathway is required when mesodermal cells start to express cardiac transcription factors.[19] In this study, we demonstrated that canonical Wnt pathway is required and sufficient for commitment of cardiomyocytes and clarified that PI3K pathway is involved in cardiomyocyte differentiation by crosstalk with canonical Wnt pathway.

Materials and Methods

Plasmids and Reagents

Constitutively active Akt (CA-Akt) and dominant negative Akt (DN-Akt) were described previously.[20] Mutant β-catenin (S33A, S37A, T41A, S45A) was from Dr S. Ishihara (Kyoto University, Japan) and Dr T. Noda (The Cancer Institute of the Japanese Foundation for Cancer Research, Japan). pGK-Wnt-3a was from Dr S. Takada (Center for Integrative Bioscience, Okazaki National Research Institutes, Japan). Constitutively active glycogen synthase kinase-3β (GSK-3β) was from Dr T. Hagen (Wolfson Digestive Diseases Centre, University Hospital Nottingham, United Kingdom). Constitutively active PI3K (myr-p110) was from Drs M. Kasuga and W. Ogawa (Kobe University, Japan). pTOPFLASH and pFOPFLASH were from Upstate biotechnology. pRL-cytomegalovirus (pRL-CMV) was from Promega. LY294002 was purchased from BioMol Research Laboratories. Akt inhibitor III was purchased from Calbiochem. Recombinant mouse Wnt-3a protein, recombinant-mouse Frizzled-8/Fc chimera protein, and recombinant insulin-like growth factor (IGF) II were purchased from R&D systems.

Cell Culture and Transfections

P19CL6 cells were cultured essentially as described previously.[19] Cells were transfected with plasmids on day 0 of differentiation using the lipofection method as previously described.[16,17] Transfection efficiency was ≈60% as examined by GFP expression plasmids (data not shown). Luciferase assay was performed essentially as described previously[21]

Immunofluorescence

For evaluating cardiomyocyte differentiation, cells were immunostained using MF20, a monoclonal antibody against sarcomeric myosin heavy chain (MHC). The cells were viewed and photographed with a confocal laser-scanning microscope (Radiance 2000; Bio-Rad). MF20 positive area was calculated and data are expressed as percentage MF20-positive area (pixel×pixel) compared with control P19CL6 cells cultured in differentiation medium.

RT-PCR

RT-PCR was performed as described previously.[19] To confirm that the obtained bands were not derived from contaminated genomic DNA, a negative experiment was done for each sample without reverse transcriptase before PCR (data not shown).

Western Blotting

Total cell lysates, cytosolic, or nuclear fractions were electrophoresed on SDS-polyacrylamide gels. Western blotting was performed as described previously.[22]

RNA Preparation and High-Density Oligonucleotide Array Hybridization

Total RNA was extracted from P19CL6 cells on days 0, 4, and 6 of DMSO-induced cardiomyocyte differentiation. Expression profiling was performed using Affymetrix GeneChip MU6500 as described previously.[23]

Statistical Analysis

Data are expressed as mean±SE. The significance of differences among means was evaluated using analysis of variance (ANOVA), followed by Fisher PLSD test and Dunnett test for multiple comparisons. Significant differences were defined as $P<0.05$.

Results

Akt Acts Downstream of PI3K in Cardiomyocyte Differentiation of P19CL6 Cells

We have recently reported that activation of PI3K is required for DMSO-induced cardiomyocyte differentiation of P19CL6 cells.[19] Akt is one of the important downstream molecules of PI3K. To clarify whether Akt activation is required for cardiomyocyte differentiation, we first examined the effects of a chemical inhibitor of Akt.[24] When the Akt inhibitor (10 μmol/L) was added to the medium through day 0 to day 4, the rate of cardiomyocyte differentiation shown by MF20 positive area was markedly decreased, although the Akt inhibitor was less effective than the PI3K inhibitor LY294002 (Figure 1A through 1C). To confirm the contribution of Akt to cardiomyocyte differentiation, we transfected a dominant negative form of Akt into P19CL6 cells. When DN-Akt was introduced into P19CL6 cells, cardiomyocyte differentiation was also suppressed (Figure 1A through 1C). We further investigated whether activation of PI3K/Akt pathway is sufficient to drive cardiomyocyte differentiation of P19CL6 cells. Myristoylated p110α, a catalytic subunit of PI3K, leads to constitutive activation of PI3K.[25] Direct activation of PI3K by transfecting this construct increased phosphorylation of Akt on Ser-473 to the same degree as DMSO treatment, indicating that PI3K signaling is activated to the same levels in these cells (Figure 1D). However, cardiomyocyte differentiation was not observed (Figure 1E). Moreover, treatment with IGF II (10 ng/mL) also increased phosphorylation of Akt but failed to induce cardiomyocyte differentiation of P19CL6 cells (Figure 1D and 1E). Furthermore, we confirmed that CA-Akt did not induce cardiomyocyte differentiation in the absence of DMSO (Figure 1C). In collection, these results suggest that PI3K/Akt pathway is necessary, but not sufficient for cardiomyocyte differentiation of P19CL6 cells.

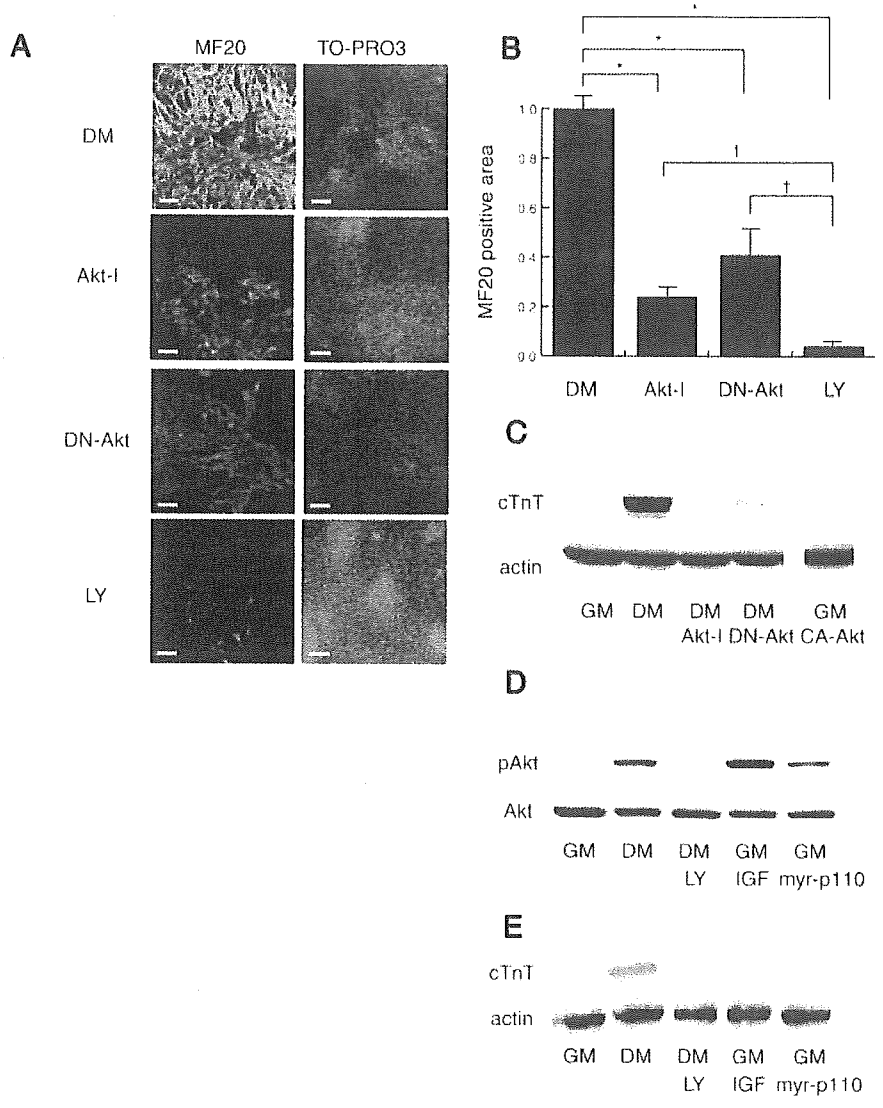

Figure 1. Akt is required, but not sufficient for cardiomyocyte differentiation. A, Suppression of cardiomyocyte differentiation by inhibiting PI3K/Akt signaling. Cells were cultured in differentiation medium (DM) to induce cardiomyocyte differentiation. On day 0, cells were transfected with DN-Akt or pcDNA3.1. LY294002 (LY) or Akt inhibitor III (Akt-I) were added to the medium for the first 4 days. Cells were stained with MF20 on day 16. Scale bars, 50 μmol/L. B, Quantification of MF20 positive area. At least 4 different fields were measured for each dish. *$P<0.001$ compared with DM. †$P<0.05$ compared with LY. C, cTnT expression, cells were cultured in DM or in growth medium (GM). On day 0, cells were transfected with DN-Akt, CA-Akt, or pcDNA3.1. Akt inhibitor III (Akt-I) was added to the medium for the first 4 days. D, Phosphorylation of Akt by IGF treatment, cells were cultured in GM or in DM. On day 0, cells were transfected with constitutively active PI3-kinase (myr-p110) or pcDNA3.1. Next day, IGF or LY294002 were added to the growth medium (IGF) or differentiation medium (LY), respectively. Cell lysates were collected 2 days after, and phosphorylation of Akt was examined by Western blotting. E, cTnT expression. IGFII or LY294002 were added from day 0 to day 4 and cTnT expression was examined on day 16 of culture.

Canonical Wnt Pathway Is Activated Transiently Only During the Early Stage of Cardiomyocyte Differentiation

To elucidate the molecular mechanisms of how PI3K/Akt pathway plays a critical role in cardiomyocyte differentiation during the early stage, we searched for the molecules that are activated during this stage, ie, through day 0 to day 4 of P19CL6 cells. By using a gene chip technology, we found that expression of *Wnt-3a* was increased 12-fold through day 0 to day 4 and decreased 5-fold by day 6 (Table). RT-PCR analysis revealed that *Wnt-3a* and *Wnt-8* but not *Wnt-1* were expressed on days 2 and 4, and TOPFLASH activity, which reflects the activity of canonical Wnt signaling, was elevated from day 0 to day 4, consistent with the expression levels of *Wnt-3a* and *Wnt-8* genes (data not shown). These results are in accordance with the previous study by Nakamura et al[18] and indicate that activation of canonical Wnt signaling occurs at the stage when PI3K/Akt signaling is required for cardiomyocyte differentiation, and suggest that canonical Wnt signaling may be a target of PI3K/Akt pathway.

Temporal Activation of Canonical Wnt Pathway Is Required and Sufficient for Cardiomyocyte Differentiation

The role of Wnt/β-catenin pathway, so-called canonical Wnt pathway, in vertebrate cardiomyocyte differentiation and

Growth Factors Expressed >3-Fold Through Day 0 to Day 4

Genbank	Gene	Days 0 to 4	Days 4 to 6
U26188	Ephrin A1	36.3	D
D12483F	Fibroblast growth factor 8 (FGF-8)	12.3	D
X56842	Wnt-3A for cysteine-rich protein	12.3	D
M22326	Early growth response 1/growth factor-induced protein (zif/268)	11.5	D
M89799	Wnt-5b	11.1	
M84607	Platelet derived growth factor receptor, alpha polypeptide	10.9	D

Growth factors whose expression levels are increased >10-fold in P19CL6 cells during day 0-day 4. D indicates decreased <3.0-fold during day 4 to day 6 or day 0 to day 6.

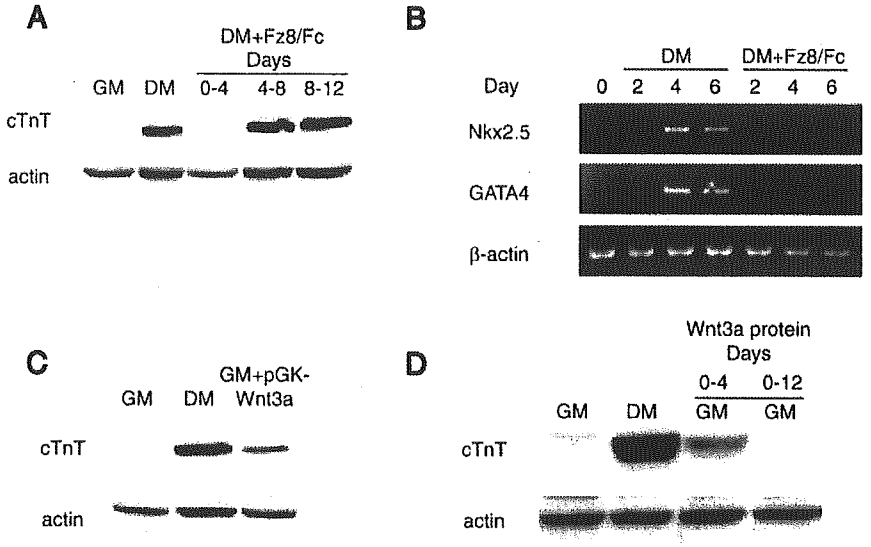

Figure 2. Temporal activation of canonical Wnt pathway is required and sufficient for cardiomyocyte differentiation of P19CL6 cells. A, Canonical Wnt activity is required for cardiomyocyte differentiation. Cells were cultured in GM or in DM. An extracellular Wnt antagonist, Fz8/Fc chimera protein was added through day 0 to 4, (0–4) 4 to 8 (4–8), and 8 to 12. (8–12). B, Changes in the expression of differentiation markers by inhibition of canonical Wnt pathway. Cells were cultured with (DM+Fz8/Fc) or without (DM) Fz8/Fc protein. RNA was collected on days 0, 2, 4, and 6, and RT-PCR analysis was performed. C, Overexpression of Wnt-3a gene induced cardiomyocyte differentiation without DMSO. Cells were cultured in GM or in DM. On day 0, cells were transfected with pGK-Wnt-3a. D, Administration of soluble Wnt protein in a specific time period (days 0 to 4, 0 to 12). Cells were cultured in growth medium and soluble Wnt-3a protein was added through day 0 to day 4 or through day 0 to day 12.

heart development is still controversial.[11–13,18] We first examined the role of canonical Wnt pathway in cardiomyocyte differentiation of P19CL6 cells. To examine whether canonical Wnt pathway is required for cardiomyocyte differentiation, we used extracellular canonical Wnt inhibitor, Fz-8/Fc chimera protein (200 ng/mL), which has been shown to inhibit canonical Wnt signaling.[26] When P19CL6 cells were treated with this protein through day 0 to day 4 of differentiation, cardiac troponin T (cTnT) was not expressed and spontaneous beating was not observed (Figure 2A), in accordance with the previous study.[18] Interestingly, when this protein was administered through day 4 to day 8, or day 8 to day 12 of differentiation, cardiomyocyte differentiation was not inhibited (Figure 2A) but spontaneous beating appeared on day 9, a day earlier than without this protein, although there were no molecular evidence, ie, difference in cTnT expression, for the appearance of earlier beating (Figure 2A and data not shown). RT-PCR analysis revealed that administration of this chimera protein from day 0 to day 4 completely abolished expression of *Nkx-2.5* and *GATA-4* (Figure 2B). These results suggest that activation of canonical Wnt signaling during the early stage is required for DMSO-induced cardiomyocyte differentiation of P19CL6 cells.

To examine whether canonical Wnt pathway is sufficient for cardiomyocyte differentiation, we first overexpressed *Wnt-3a* cDNA in P19CL6 cells and cultured them in growth medium without DMSO. P19CL6 cells expressed cTnT (Figure 2C) and showed spontaneous contraction after 10 days of culture. Next, we cultured P19CL6 cells in growth medium with soluble Wnt-3a protein (100 ng/mL, R&D systems). Surprisingly, when soluble Wnt-3a protein was added to the growth medium continuously, cells never started spontaneous contraction nor expressed cTnT (Figure 2D). However, when the protein was added only during the first 4 days of culture, when canonical Wnt pathway is activated endogenously in DMSO-treated P19CL6 cells, spontaneous contraction was observed from day 10 and cells expressed cTnT (Figure 2D). These results suggest that canonical Wnt signaling has 2 different roles in cardiomyocyte differentiation depending on the differentiation stage of the cells. Although the canonical Wnt pathway promotes commitment into cardiac lineage at the early stage, it inhibits further differentiation into mature cardiomyocytes at the later stage.

PI3K/Akt Pathway Maintains Canonical Wnt Activity Through GSK-3β During DMSO-Induced Cardiomyocyte Differentiation of P19CL6 Cells

Because canonical Wnt pathway plays an essential role in cardiomyocyte differentiation when PI3K/Akt pathway is required for cardiomyocyte differentiation, we hypothesized that PI3K/Akt pathway is required for the activation of canonical Wnt pathway. To test our hypothesis, we first examined whether CA- or DN-Akt could affect canonical Wnt activity in P19CL6 cells. Consistent with previous studies,[27,28] introduction of CA-Akt or DN-Akt did not change canonical Wnt activity (assessed by TOPFLASH activity) in undifferentiated P19CL6 cells (Figure 3A). Introduction of Akt constructs did not change TOPFLASH activity in L-fibroblasts, NIH3T3 cells, and COS-7 cells (data not shown). However, when P19CL6 cells were treated with DMSO and induced to differentiate into cardiomyocytes, TOPFLASH activity was enhanced by CA-Akt and suppressed by DN-Akt (Figure 3A). These observations indicate that it depends on cell types whether PI3K/Akt pathway activates canonical Wnt pathway or not.

GSK-3β, a ubiquitously-expressed constitutively-active serine/threonine kinase, regulates a wide variety of cellular

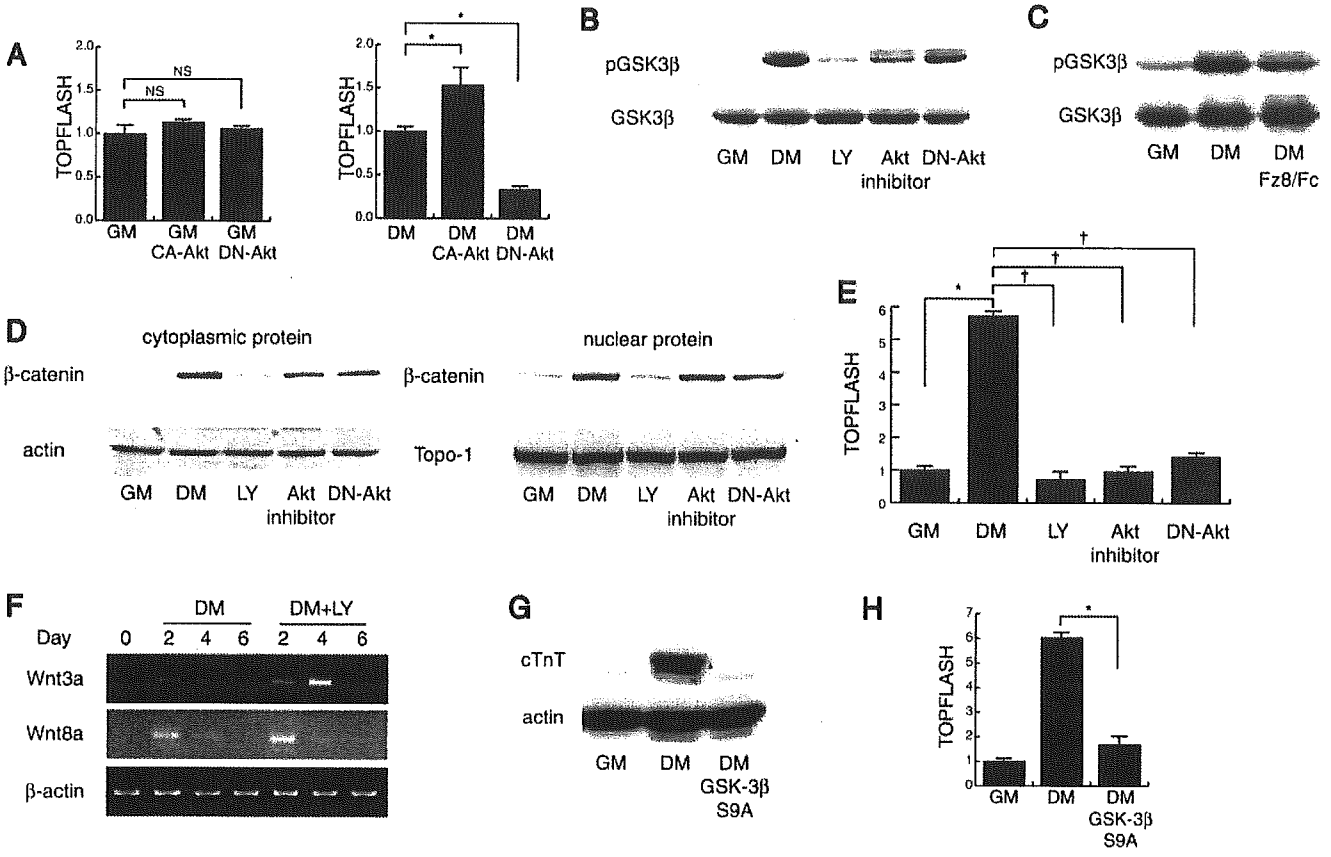

Figure 3. PI3K/Akt pathway changes canonical Wnt activity through GSK-3β in differentiation-induced P19CL6 cells. A, Canonical Wnt activity is altered by PI3K/Akt activity only when cells were treated with DMSO. Cells were cultured in GM or in DM. On day 0, cells were transfected with pTOPFLASH, pRL-CMV, together with or without CA-Akt or DN-Akt. NS, not significant. *$P<0.001$ compared with DM. B, Phosphorylation of GSK-3β in P19CL6 cells by inhibition of PI3K/Akt pathway. Cells were cultured in GM or in DM. On day 0, cells were transfected with DN-Akt or pcDNA3.1. Cells were cultured until day 4, and phosphorylation of GSK-3β was examined by Western blotting. C, Phosphorylation of GSK-3β by addition of Fz8/Fc chimera protein. D, β-catenin expression in P19CL6 cells by inhibition of PI3K/Akt pathway. Cells were cultured as described in Figure 3B and fractionated into cytoplasmic and nuclear fraction. Expression of β-catenin was examined by Western blotting. The same membrane was stripped and labeled with anti-actin (for cytoplasmic fraction) or anti–Topo-1 (nuclear fraction) antibodies to verify even sample loading. D, TOPFLASH activity in P19CL6 cells by inhibition of PI3K/Akt pathway. On day 0, cells were transfected with DN-Akt or pcDNA3.1, pTOPFLASH and pRL-CMV for control. After transfection, medium was changed to GM, DM (DM, DN-Akt), or DM containing LY294002 (LY) or Akt inhibitor III (Akt inhibitor). *$P<0.001$ compared with GM. †$P<0.001$ compared with DM. E, Expression levels of Wnt-3a and Wnt-8 genes after inhibition of PI3K pathway. Cells were cultured in a DM in the presence (DM+LY) or absence (DM) of PI3K inhibitor, LY294002. RNA was extracted on days 0, 2, 4, and 6, and expression of Wnt-3a and Wnt-8 genes was analyzed by RT-PCR. F, Akt phosphorylation-insensitive mutant GSK-3β blocked cardiomyocyte differentiation. Cells were cultured in GM or in DM. On day 0, cells were transfected with constitutively-active GSK-3β (GSK-3β S9A) or with pcDNA3.1. G, TOPFLASH activity in P19CL6 cells by GSK-3β S9A. Cells were cultured as described in Figure 4F. On day 0, cells were transfected with GSK-3β S9A or pcDNA3.1, pTOPFLASH, and pRL-CMV for control. After transfection, medium was changed to GM or DM (DM, GSK-3β S9A). *$P<0.001$ compared with DM.

functions downstream of signaling pathways including PI3K/Akt pathway and canonical Wnt pathway.[29] GSK-3β activity is suppressed by phosphorylation at the Ser-9 by Akt.[30] On the other hand, GSK-3β phosphorylates and promotes degradation of β-catenin and downregulates canonical Wnt signaling. By the treatment with DMSO, phosphorylation of GSK-3β was increased and this increase was suppressed by inhibiting PI3K/Akt pathway both chemically and genetically (Figure 3B). Inhibition of canonical Wnt signaling by Fz-8/Fc protein only slightly decreased GSK-3β phosphorylation that is increased by DMSO treatment (Figure 3C), whereas it severely decreased cardiomyocyte differentiation. This result suggests that canonical Wnt pathway does not directly interact with PI3K/Akt pathway, and thus we speculate that activation of PI3K/Akt and the following phosphorylation of GSK-3β by DMSO is not mediated via canonical Wnt signaling. However, further analyses are required to elucidate whether canonical Wnt pathway and PI3K/Akt pathway interact directly or not. Inhibition of PI3K/Akt pathway and phosphorylation of GSK-3β decreased expression levels of cytoplasmic and nuclear β-catenin (Figure 3D), and the TOPFLASH activity (Figure 3E) in DMSO treated P19CL6 cells. Inhibition of PI3K/Akt pathway did not alter the expression levels of Wnt-3a and Wnt-8 genes (Figure 3F), indicating that the decrease in the canonical Wnt activity is not attributable to decreased expression levels of Wnt-3a or Wnt-8. To further examine whether decreased cardiomyocyte differentiation by PI3K/Akt pathway inhibition is attributable to decreased Ser-9 phosphorylation of GSK-3β, we overexpressed GSK-3β whose Ser-9 is substituted into alanine and

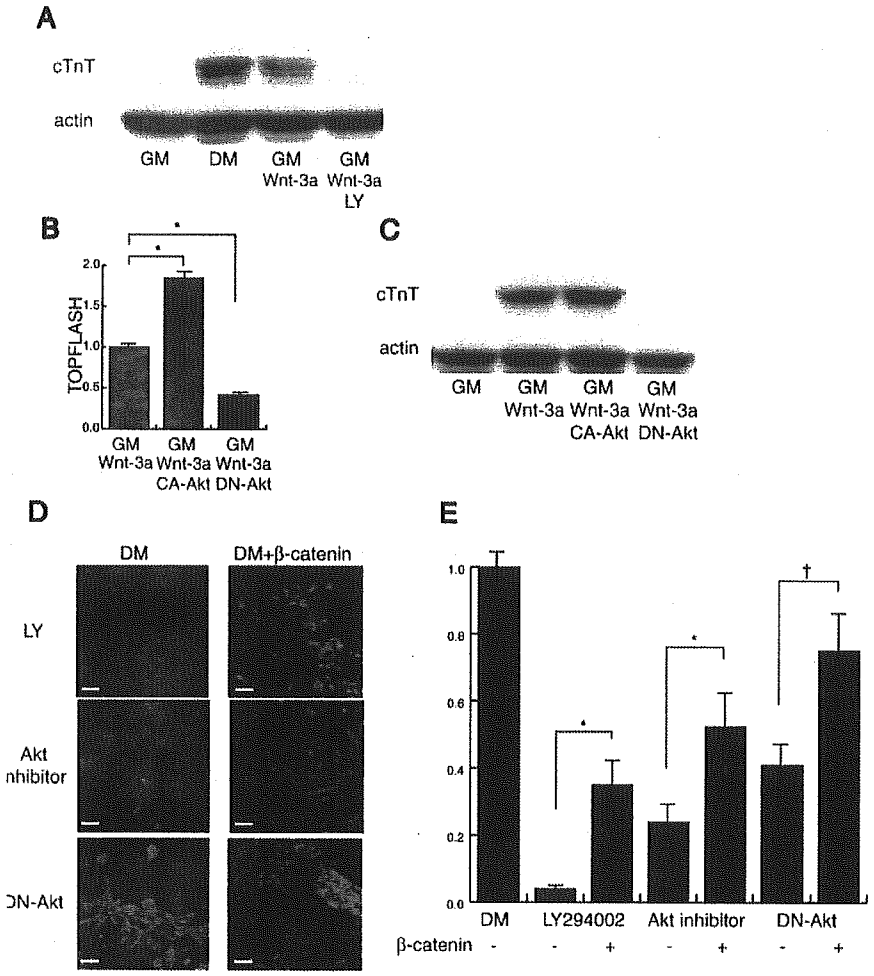

Figure 4. PI3K/Akt pathway and canonical Wnt pathway act synergistically to induce cardiomyocyte differentiation in P19CL6 cells. A, LY294002 inhibited soluble Wnt protein-induced cardiomyocyte differentiation. Cells were cultured in GM or in DM. Soluble Wnt-3a protein was added to the growth medium with or without LY294002 through day 0 to day 4. B, Akt activity correlates with canonical Wnt activity in Wnt-3a transfected P19CL6 cells. Cells were cultured in GM. On day 0, cells were transfected with pTOPFLASH, pRL-SV40, pcDNA3.1 (GM), and pGK-Wnt-3a (Wnt-3a) together with or without CA-Akt or DN-Akt. *$P<0.001$ compared with GM Wnt-3a. C, cTnT expression. Cells were cultured in growth medium. On day 0, cells were transfected with pGK-Wnt-3a (Wnt-3a) together with CA-Akt or DN-Akt. D, Suppression of cardiomyocyte differentiation by inhibiting PI3K/Akt signaling was rescued by activating canonical Wnt pathway. Cells were cultured as described in Figure 1A. On day 0, cells were transfected with DN-Akt or pcDNA3.1, together with or without mutant β-catenin. Cells were stained with MF20 on day 16. Scale bars, 50 μmol/L. E, Quantification of MF20-positive area. At least 4 different fields were measured for each dish. *$P<0.05$, †$P<0.01$ compared with mutant β-catenin nontransfected counterparts.

insensitive to Akt phosphorylation.[31] Introduction of this mutant protein into P19CL6 cells on day 0 completely abrogated DMSO-induced cardiomyocyte differentiation and DMSO-induced elevation of TOPFLASH activity (Figure 3G and 3H). These results suggest that when P19CL6 cells are induced to differentiate into cardiomyocytes, PI3K/Akt pathway, activated independently of canonical Wnt signaling, is required to maintain canonical Wnt activity by suppressing GSK-3β.

PI3K/Akt Pathway and Canonical Wnt Pathway Synergistically Induce Cardiomyocyte Differentiation

If inhibition of PI3K/Akt pathway decreases DMSO-induced cardiomyocyte differentiation in P19CL6 cells by regulating GSK-3β activity, inhibition of PI3K/Akt pathway should also affect Wnt-3a–induced cardiomyocyte differentiation in P19CL6 cells. To test this, we cultured P19CL6 cells in growth medium with soluble Wnt-3a protein and LY294002 for the first 4 days. Cardiomyocyte differentiation induced by soluble Wnt-3a protein was completely blocked by LY294002 treatment (Figure 4A). We next cotransfected CA-Akt or DN-Akt with pGK-Wnt-3a in P19CL6 cells. As expected, cotransfection of CA-Akt and Wnt-3a elevated TOPFLASH activity and expression levels of cTnT. To the contrary, DN-Akt suppressed Wnt-3a–induced increase in TOPFLASH activity and completely blocked cardiomyocyte differentiation (Figure 4B). Finally, we introduced mutant β-catenin, which is insensitive to phosphorylation by GSK-3β, into P19CL6 cells, and examined whether this could rescue cardiomyocyte differentiation of P19CL6 cells. Introduction of the mutant β-catenin restored cardiomyocyte differentiation, which was suppressed by inhibition of PI3K/Akt pathway (Figure 4C through 4E). These results suggest that PI3K/Akt pathway is required to maintain certain levels of canonical Wnt activity that is enough to induce cardiomyocyte differentiation of P19CL6 cells.

Discussion

In this study, we elucidated the molecular mechanism by which PI3K is critically involved in cardiomyocyte differentiation in vitro. Akt, which was activated by the DMSO treatment, was required for cardiomyocyte differentiation of P19CL6 cells as a downstream of PI3K. Canonical Wnt pathway regulated cardiomyocyte differentiation positively and negatively, depending on the stage of differentiation. Inhibition of PI3K/Akt pathway decreased the content of cytoplasmic and nuclear β-catenin and the activity of canonical Wnt pathway through decreased GSK-3β phosphorylation.

Many studies have indicated that PI3K is involved in the differentiation of various kinds of cells such as myoblasts,[32] osteoblasts,[33] and adipocytes.[34] In this study, Akt was in-

volved in cardiomyocyte differentiation downstream of PI3K. However, introduction of myristoylated, constitutively-active form of Akt could not induce cardiomyocyte differentiation of P19CL6 cells in the absence of DMSO (Figure 1E), suggesting that activation of Akt pathway is required, but not sufficient for cardiomyocyte differentiation.

PI3K/Akt pathway affected cardiomyocyte differentiation through maintaining the activity of the canonical Wnt pathway. Activation of the canonical Wnt pathway was required and sufficient for induction of cardiac transcription factors and cardiomyocyte differentiation in P19CL6 cells. It is noteworthy that this positive regulation of cardiomyocyte differentiation by the canonical Wnt pathway is only temporal, and prolonged activation of canonical Wnt pathway rather inhibited full differentiation into spontaneously contracting cardiomyocytes (Figure 3D). Using *Xenopus* and chick embryos, it has been reported that inhibitors of canonical Wnt signaling such as *crescent* and *Dkk-1* are secreted from anterior mesoderm and induce cardiogenesis and that ectopic stimulation of canonical Wnt signaling in this area inhibited cardiomyocyte differentiation.[11–13] In those studies, expression of *Wnt-3a* and *Wnt-8*, which is transiently observed in all embryonic mesoderm,[35] is already limited to posterior mesoderm and is not observed in the anterior mesoderm. The stage when canonical Wnts are expressed corresponds to day 4 or earlier of P19CL6 cell differentiation, indicating that our findings do not contradict with the previous in vivo studies.[11–13] Prolonged exposure to canonical Wnt signaling rather blocked full differentiation into spontaneously contracting cardiomyocyte (Figure 3D). Nakamura et al have reported that canonical Wnt pathway contributes positively to cardiomyocyte differentiation,[18] which is consistent with our results. However, there is some difference between the 2 studies. Activation of the canonical Wnt pathway was sufficient for differentiation into mature spontaneously-contracting cardiomyocytes in our study but not in their study. This discrepancy may come from the duration of Wnt-3a stimulation. We limited the Wnt-3a stimulation to initial 4 days of P19CL6 cell differentiation because thereafter Wnt-3a activation inhibited cardiomyocyte differentiation (Figure 3D). Collectively, our results may explain contradicting results on the requirement of canonical Wnt pathway between in vivo[11–13] and in vitro[18] experiments. Further studies are necessary to elucidate the mechanism of how canonical Wnt pathway shows such biphasic roles in cardiomyocyte differentiation by a differentiation stage-specific manner.

It is still on debate whether canonical Wnt pathway and PI3K/Akt pathway interact with each other through regulation of GSK-3β.[36] Previous reports showed that PI3K/Akt pathway and canonical Wnt pathway is pharmacologically distinct.[27,28] In our study, we observed that PI3K/Akt pathway itself did not activate canonical Wnt pathway but was required for maintenance of canonical Wnt pathway. Our observations do not contradict to previous reports from the point that both signalings are independent and one cannot activate the other pathway. Moreover, Yuan et al[27] showed the synergism between PI3K/Akt pathway and canonical Wnt pathway when both signaling pathways are activated, which

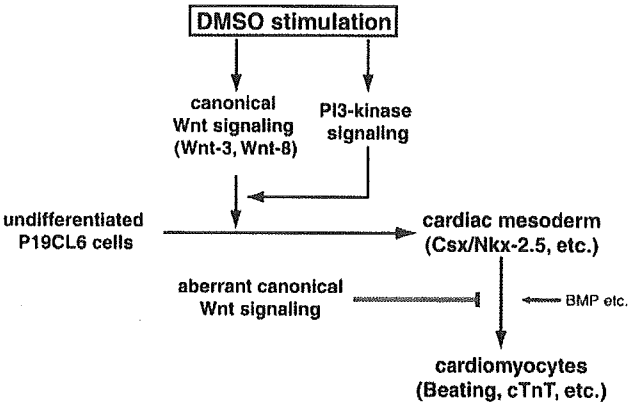

Figure 5. Regulation of early cardiomyogenesis by PI3K and the canonical Wnt pathway. After DMSO treatment, undifferentiated P19CL6 cells start to differentiate into cardiac mesodermal cells and mature cardiomyocytes. DMSO treatment activates both the canonical Wnt pathway and the PI3K pathway independently. Activation of the canonical Wnt pathway is required and sufficient for induction of cardiac mesodermal cells. During cardiac mesoderm induction, PI3K pathway enhances activity of the canonical Wnt pathway and both pathways act together in commitment of cardiac mesodermal cells. Once committed into cardiac mesodermal cells, aberrant activation of canonical Wnt signaling rather suppressed further maturation into functional cardiomyocytes.

is consistent with our study (Figures 4A and 5B). In addition, a growing body of evidence suggests that there is a synergistic effect between PI3K/Akt pathway and canonical Wnt pathway in differentiating neuronal cells,[37] intestinal cells,[38] and myoblasts.[39] We speculate that synergistic action between PI3K/Akt pathway and canonical Wnt pathway exists in certain circumstances such as during differentiation of cells or development of organs.

It should be noted that PI3K/Akt pathway may act as a survival factor for the cardiac mesodermal cells during DMSO- and Wnt-induced cardiomyocyte differentiation in P19CL6 cells in addition to its activity to maintain canonical Wnt activity during cardiomyocyte differentiation.

In summary, we elucidated the molecular mechanisms of how PI3K signaling affects cardiomyocyte differentiation (Figure 5). Canonical Wnt pathway plays a primary and pivotal role in initiation of cardiomyocyte differentiation, and PI3K pathway plays an important role in cardiomyocyte differentiation by maintaining canonical Wnt activity. It is also noteworthy that canonical Wnt pathway is required only temporally and plays both positive and negative roles in cardiomyocyte differentiation by the differentiation stage-dependent manner. Our novel findings in this study could explain contradictory reports between in vitro and in vivo on the role of canonical Wnt pathway in cardiomyocyte differentiation.

Acknowledgments

This work was supported in part by grants from the Japanese Ministry of Education, Science, Sports, and Culture; Japan Health Sciences Foundation; Takeda Medical Research Foundation; Takeda Science Foundation; Uehara Memorial Foundation; Kato Memorial Trust for Nambyo Research; Japan Medical Association (to I.K.); Japanese Heart Foundation/Pfizer Japan Grant on Cardiovascular Disease Research; Takeda Science Foundation (to H.A.); Japan

Heart Foundation Young Investigator's Research Grant (to A.T.N.). We thank E. Fujita, A. Furuyama, M. Ikeda, R. Kobayashi, and Y. Ohtsuki for their excellent technical assistance, and Drs S. Ishihara, T. Noda, S. Takada, T. Hagen, W. Ogawa, and M. Kasuga for providing us plasmids.

References

1. Kinder SJ, Tsang TE, Wakamiya M, Sasaki H, Behringer RR, Nagy A, Tam PP. The organizer of the mouse gastrula is composed of a dynamic population of progenitor cells for the axial mesoderm. *Development.* 2001;128:3623–3634.
2. Watson CM, Tam PP. Cell lineage determination in the mouse. *Cell Struct Funct.* 2001;26:123–129.
3. Fishman MC, Chien KR. Fashioning the vertebrate heart: earliest embryonic decisions. *Development.* 1997;124:2099–2117.
4. Olson EN, Schneider MD. Sizing up the heart: development redux in disease. *Genes Dev.* 2003;17:1937–1956. Epub 2003 Jul 31.
5. Schultheiss TM, Burch JB, Lassar AB. A role for bone morphogenetic proteins in the induction of cardiac myogenesis. *Genes Dev.* 1997;11: 451–462.
6. Alsan BH, Schultheiss TM. Regulation of avian cardiogenesis by Fgf8 signaling. *Development.* 2002;129:1935–1943.
7. Shi Y, Katsev S, Cai C, Evans S. BMP signaling is required for heart formation in vertebrates. *Dev Biol.* 2000;224:226–237.
8. Walters MJ, Wayman GA, Christian JL. Bone morphogenetic protein function is required for terminal differentiation of the heart but not for early expression of cardiac marker genes. *Mech Dev.* 2001;100:263–273.
9. Cadigan KM, Nusse R. Wnt signaling: a common theme in animal development. *Genes Dev.* 1997;11:3286–3305.
10. Park M, Wu X, Golden K, Axelrod JD, Bodmer R. The wingless signaling pathway is directly involved in Drosophila heart development. *Dev Biol.* 1996;177:104–116.
11. Marvin MJ, Di Rocco G, Gardiner A, Bush SM, Lassar AB. Inhibition of Wnt activity induces heart formation from posterior mesoderm. *Genes Dev.* 2001;15:316–327.
12. Schneider VA, Mercola M. Wnt antagonism initiates cardiogenesis in Xenopus laevis. *Genes Dev.* 2001;15:304–315.
13. Tzahor E, Lassar AB. Wnt signals from the neural tube block ectopic cardiogenesis. *Genes Dev.* 2001;15:255–260.
14. Veeman MT, Axelrod JD, Moon RT. A second canon. Functions and mechanisms of beta-catenin-independent Wnt signaling. *Dev Cell.* 2003; 5:367–377.
15. Pandur P, Lasche M, Eisenberg LM, Kuhl M. Wnt-11 activation of a non-canonical Wnt signalling pathway is required for cardiogenesis. *Nature.* 2002;418:636–641.
16. Monzen K, Shiojima I, Hiroi Y, Kudoh S, Oka T, Takimoto E, Hayashi D, Hosoda T, Habara-Ohkubo A, Nakaoka T, Fujita T, Yazaki Y, Komuro I. Bone morphogenetic proteins induce cardiomyocyte differentiation through the mitogen-activated protein kinase kinase kinase TAK1 and cardiac transcription factors Csx/Nkx-2.5 and GATA-4. *Mol Cell Biol.* 1999;19:7096–7105.
17. Monzen K, Hiroi Y, Kudoh S, Akazawa H, Oka T, Takimoto E, Hayashi D, Hosoda T, Kawabata M, Miyazono K, Ishii S, Yazaki Y, Nagai R, Komuro I. Smads, TAK1, and their common target ATF-2 play a critical role in cardiomyocyte differentiation. *J Cell Biol.* 2001;153:687–698.
18. Nakamura T, Sano M, Songyang Z, Schneider MD. A Wnt- and beta -catenin-dependent pathway for mammalian cardiac myogenesis. *Proc Natl Acad Sci U S A.* 2003;100:5834–5839. Epub 2003 Apr 28.
19. Naito AT, Tominaga A, Oyamada M, Oyamada Y, Shiraishi I, Monzen K, Komuro I, Takamatsu T. Early stage-specific inhibitions of cardiomyocyte differentiation and expression of Csx/Nkx-2.5 and GATA-4 by phosphatidylinositol 3-kinase inhibitor LY294002. *Exp Cell Res.* 2003; 291:56–69.
20. Miyauchi H, Minamino T, Tateno K, Kunieda T, Toko H, Komuro I. Akt negatively regulates the in vitro lifespan of human endothelial cells via a p53/p21-dependent pathway. *EMBO J.* 2004;23:212–220. Epub 2004 Jan 08.
21. Akazawa H, Kudoh S, Mochizuki N, Takekoshi N, Takano H, Nagai T, Komuro I. A novel LIM protein Cal promotes cardiac differentiation by association with CSX/NKX2–5. *J Cell Biol.* 2004;164:395–405.
22. Zhu W, Shiojima I, Hiroi Y, Zou Y, Akazawa H, Mizukami M, Toko H, Yazaki Y, Nagai R, Komuro I. Functional analyses of three Csx/Nkx-2.5 mutations that cause human congenital heart disease. *J Biol Chem.* 2000; 275:35291–35296.
23. Mizukami M, Hasegawa H, Kohro T, Toko H, Kudoh S, Zou Y, Aburatani H, Komuro I. Gene expression profile revealed different effects of angiotensin II receptor blockade and angiotensin-converting enzyme inhibitor on heart failure. *J Cardiovasc Pharmacol.* 2003;42:S1–S66.
24. Kozikowski AP, Sun H, Brognard J, Dennis PA. Novel PI. Analogues selectively block activation of the pro-survival serine/theonine kinase Akt. *J Am Chem Soc.* 2003;125:1144–1145.
25. Kitamura T, Kitamura Y, Kuroda S, Hino Y, Ando M, Kotani K, Konishi H, Matsuzaki H, Kikkawa U, Ogawa W, Kasuga M. Insulin-induced phosphorylation and activation of cyclic nucleotide phosphodiesterase 3B by the serine-threonine kinase Akt. *Mol Cell Biol.* 1999;19:6286–6296.
26. Hsieh JC, Rattner A, Smallwood PM, Nathans J. Biochemical characterization of Wnt-frizzled interactions using a soluble, biologically active vertebrate Wnt protein. *Proc Natl Acad Sci U S A.* 1999;96:3546–3551.
27. Yuan H, Mao J, Li L, Wu D. Suppression of glycogen synthase kinase activity is not sufficient for leukemia enhancer factor-1 activation. *J Biol Chem.* 1999;274:30419–30423.
28. Ding VW, Chen RH, McCormick F. Differential regulation of glycogen synthase kinase 3beta by insulin and Wnt signaling. *J Biol Chem.* 2000; 275:32475–32481.
29. Harwood AJ. Regulation of GSK-3: a cellular multiprocessor. *Cell.* 2001; 105:821–824.
30. Cross DA, Alessi DR, Cohen P, Andjelkovich M, Hemmings BA. Inhibition of glycogen synthase kinase-3 by insulin mediated by protein kinase B. *Nature.* 1995;378:785–789.
31. Hagen T, Di Daniel E, Culbert AA, Reith AD. Expression and characterization of GSK-3 mutants and their effect on beta-catenin phosphorylation in intact cells. *J Biol Chem.* 2002;277:23330–23335. Epub 2002 Apr 19.
32. Jiang BH, Aoki M, Zheng JZ, Li J, Vogt PK. Myogenic signaling of phosphatidylinositol 3-kinase requires the serine-threonine kinase Akt/ protein kinase B. *Proc Natl Acad Sci U S A.* 1999;96:2077–2081.
33. Ghosh-Choudhury N, Abboud SL, Nishimura R, Celeste A, Mahimainathan L, Choudhury GG. Requirement of BMP-2-induced phosphatidylinositol 3-kinase and Akt serine/threonine kinase in osteoblast differentiation and Smad-dependent BMP-2 gene transcription. *J Biol Chem.* 2002;277:33361–33368. Epub 2002 Jun 25.
34. Magun R, Burgering BM, Coffer PJ, Pardasani D, Lin Y, Chabot J, Sorisky A. Expression of a constitutively activated form of protein kinase B (c-Akt) in 3T3–L1 preadipose cells causes spontaneous differentiation. *Endocrinology.* 1996;137:3590–3593.
35. Takada S, Stark KL, Shea MJ, Vassileva G, McMahon JA, McMahon AP. Wnt-3a regulates somite and tailbud formation in the mouse embryo. *Genes Dev.* 1994;8:174–189.
36. Brazil DP, Park J, Hemmings BA. PKB binding proteins. Getting in on the Akt. *Cell.* 2002;111:293–303.
37. Fukumoto S, Hsieh CM, Maemura K, Layne MD, Yet SF, Lee KH, Matsui T, Rosenzweig A, Taylor WG, Rubin JS, Perrella MA, Lee ME. Akt participation in the Wnt signaling pathway through Dishevelled. *J Biol Chem.* 2001;276:17479–17483. Epub 2001 Mar 9.
38. He XC, Zhang J, Tong WG, Tawfik O, Ross J, Scoville DH, Tian Q, Zeng X, He X, Wiedemann LM, Mishina Y, Li L. BMP signaling inhibits intestinal stem cell self-renewal through suppression of Wnt-beta-catenin signaling. *Nat Genet.* 2004;36:1117–1121. Epub 2004 Sep 19.
39. Rochat A, Fernandez A, Vandromme M, Moles JP, Bouschet T, Carnac G, Lamb NJ. Insulin and wnt1 pathways cooperate to induce reserve cell activation in differentiation and myotube hypertrophy. *Mol Biol Cell.* 2004;15:4544–4555. Epub 2004 Jul 28.